

**Biotransformations of Water Insoluble Substrates in
Aqueous, Two-Phase and Encapsulated Systems**

By
DIANA IEZZI, B.Sc.

A Thesis Submitted to the Department of Chemistry in
Partial Fulfillment of the Requirements for the
Degree of
Master of Science

Brock University
August, 1999

©

Abstract

The biotransformation of water insoluble substrates by mammalian and bacterial cells has been problematic, since these whole cell reactions are primarily performed in an aqueous environment. The implementation of a two-phase or encapsulated system has the advantages of providing a low water system along with the physiological environment the cells require to sustain themselves. Encapsulation of mammalian cells by formation of polyamide capsules via interfacial polymerization illustrated that the cells could not survive this type of encapsulation process. Biotransformation of the steroid spironolactone [3] by human kidney carcinoma cells was performed in a substrate-encapsulated system, yielding canrenone [4] in 70% yield.

Encapsulation of nitrile-metabolizing *Rhodococcus rhodochrous* cells using a polyamide membrane yielded leaky capsules, but biotransformation of 2-(4-chlorophenyl)-3-methylbutyronitrile (CPIN) [6] in a free cell system yielded CPIN amide [7] in 40% yield and 94% ee. A two-phase biotransformation of CPIN consisting of a 5:1 ratio of tris buffer, pH 7.2 to octane respectively, gave CPIN acid [8] in 30% yield and 97% ee. It was concluded that *Rhodococcus rhodochrous* ATCC 17895 contained a nonselective nitrile hydratase and a highly selective amidase enzyme.

Acknowledgments

I would like to acknowledge my supervisor, Dr. H.L. Holland for his guidance and insightful contributions to this work.

A special thanks goes out to Gino Stroffolino for his practical experience pertaining to this work, which he handed down to me.

To Donna Vukmanic, for her willingness to teach me how to use the GC machine, to Dr. Fred Capretta for his analysis work on his new chiral GC machine, which nobody else can touch, and to Mr. Tim Jones for performing all mass spectral analyses, I thank you all.

To my supervisory committee, Dr. Brennan, Dr. Haj-Amad, and Dr. Atkinson, and Dr. Legge for their time and helpful suggestions.

To all my friends at Brock University, especially everyone in H221 and H224 for a wonderful time.

And last but never least, all of my family (old and new) for their encouragement and enlightenment.

	PAGE
ABSTRACT	
Acknowledgments	iii
TABLE OF CONTENTS	
CHAPTER 1: INTRODUCTION	
1.0 Interfacial Polymerization	2
1.1 Applications of Encapsulated Systems	7
1.2 Two-phase Systems	12
1.3 <i>Rhodococcus rhodochrous</i> Biotransformation of Nitriles	18
1.3.1 Substrate Specificity of Nitrile Hydratase and Amidase	20
1.3.2 Mechanisms of Nitrile Hydratase	25
1.3.3 Mechanism of Amidases	28
1.4 Mammalian Cell Metabolism	30
CHAPTER 2: EXPERIMENTAL	
2.1 Mammalian Cell Culture Project	
2.1.1 Cell Cultivation	37
Mouse Liver Cells	
Human Kidney Carcinoma Cells	
2.1.2 Encapsulation Methodology	39
Method 1: Encapsulation of Mammalian Cells	
Method 2: Encapsulation of Substrate	
Method 3: Encapsulation of Substrate with Dialysis Tubing	
2.1.3 Viability Studies	42
Capsule Disruption	
Viability via Biotransformation	
Viability Staining	
2.1.4 Bioreactor	45
Assembly to Inoculation	
2.1.5 Biotransformation	51
Biotransformation Conditions	
2.1.6 Product Recovery	52
Medium Manipulation	
Product Isolation	
2.1.7 Toxicity Assays	54
Pharmaceutical Thresholds	
Optimal Reagent Concentrations for Encapsulation	

2.1.8 Preparation of Starting Material Pyrilamine Free Base	56
2.2 <i>Rhodococcus rhodochrous</i> Project	
2.2.1 Growth Conditions	57
<i>Rhodococcus rhodochrous</i>	
2.2.2 Free Cell Biotransformation	58
Heptyl Nitrile	
CPIN	
2.2.3 Two-Phase Biotransformation	59
Heptyl Nitrile	
CPIN	
2.2.4 Encapsulated Biotransformation	59
Heptyl Nitrile	
CPIN	
2.2.5 Viability Studies	60
2.2.6 GC Analysis	61
Description	
Heptyl Nitrile Analysis Conditions	
CPIN Analysis Conditions	
2.2.7 Product Recovery and Isolation	62
2.2.8 Preparation of Materials	63
Synthesis of Octyl Amide	
Synthesis of CPIN via Grignard Reaction	
Synthesis of CPIN using Industrial Approach	
Synthesis of CPIN acid	
Derivatization of CPIN acid to methyl ester	
2.2.9 Chiral Analysis	67
 CHAPTER 3: RESULTS AND DISCUSSION	
3.1 Mammalian Cell Culture Project	
3.1.1 Encapsulation of Mammalian Cells	69
3.1.2 Viability Determination	74
Capsule Disruption	
Biotransformation	
Viability Staining	
3.1.3 Reverse Capsule Formation	80
3.1.4 Encapsulation Using Dialysis Tubing	83
Bioconversion of Chloramphenicol	
Bioconversion of Spironolactone	
3.2 <i>Rhodococcus rhodochrous</i> Project	
3.2.1 Optimization of Growth Conditions	89

3.2.2 Heptyl Nitrile Biotransformation	91
Free Cell	
Two-phase	
Encapsulated	
3.2.3 CPIN Biotransformation	97
Synthesis of CPIN	
Free Cell Biotransformation	
Two-phase Biotransformation	
3.2.4 Chiral Analysis of CPIN biotransformation	105
 CONCLUSIONS AND FUTURE WORK	 108
 REFERENCES	 112

LIST OF FIGURES AND TABLES	PAGE
Figure 1: Methodology of interfacial polymerization	3
Figure 2: Monomers used for interfacial polymerization	5
Figure 3: Biotransformation of 1-phenyl-1-2propanedione	8
Figure 4: Biotransformation of propionitrile	12
Figure 5: Biocatalysis of hydrocortisone	14
Figure 6: Conversion of feurulic acid to 4-vinyl guaicol	15
Figure 7: Chemical hydrolysis of nitriles	18
Figure 8: Enzymatic hydrolysis of nitriles	19
Figure 9: Substrate selectivity of nitrile hydratase and amidase	21
Figure 10: Biotransformation of a nitrile to give ibuprofen	23
Figure 11: Scheme of hydrolysis of CPIN by <i>Pseudomonas sp.</i>	24
Figure 12: Possible scheme for NO-dependent photoactivity	26
Figure 13: Mechanism of nitrile hydratase	27
Figure 14: Proposed mechanism for amidase reaction	29
Table 1: Reactions of phase I and phase II metabolism	31
Figure 15: Cyt-P450 protoporphyrin IX	32
Figure 16: Cyt-P450 cycle in drug oxidations	33
Figure 17: Hydroxylation of androst-4-ene-3,17-dione	34
Figure 18: Metabolism of norgestrel by Cyt-P450	35

Figure 19A: S-oxidation of thioridazine	36
Figure 19B: N-demethylation of diazepam	36
Scheme 1: Flow chart for interfacial polymerization	39
Figure 20: Schematic of Celligen	46
Table 3: Results from MOPS toxicity assay	70
Table 4: Quantities of reagents for encapsulation of yeast cells	71
Table 5: Quantities of reagents for encapsulation of mammalian cells	72
Figure 21: Microencapsulated human cells under a light microscope	73
Table 6: Toxicity assay for pyrilamine maleate	77
Table 7: Results of viability staining for mouse liver cells	79
Figure 22: Reverse phase capsules as seen under an electron microscope	82
Table 8: Viability of mouse cells in the presence solvents in dialysis tubing	84
Table 9: Solubility of pharmaceuticals in organic solvents and water	85
Scheme 7: Mechanism for biotransformation of spironolactone	88
Figure 23A: Free cell conversion of heptyl nitrile	92
Figure 23B: Frozen free cell conversion of heptyl nitrile	92
Figure 24A: Organic phase of heptyl nitrile conversion	95
Figure 24B: Aqueous phase of heptyl nitrile conversion	95
Scheme 8: Mechanism for synthesis of CPIN using Grignard reaction	97
Scheme 9: Synthesis of CPIN using industrial approach	98

Figure 25: Conversion of CPIN in free cell system	102
Figure 26A: Aqueous phase of CPIN conversion	104
Figure 26B: Organic phase of CPIN conversion	104
Table 10: Results of chiral analysis of CPIN and products	106
Figure 27A: Enantiomeric peaks for chiral analysis of CPINamide	107
Figure 27B: Enantiomeric analysis of CPIN acid	108

Chapter 1: Introduction

The advantages of using enzymes and whole cell systems for biotransformation of substrates has long been recognized in organic synthesis. One of the most successful biocatalytic applications is the industrial production of acrylamide from acrylonitrile by *Rhodococcus rhodochrous* J1, which yields 30,000 tons of acrylamide per year (1). The implementation of this bacterial transformation improved productivity due to the high activity of the enzyme involved, which in turn eliminated side reactions and by-products formed by chemical means. In addition, less downstream processing and mild conditions made the process more economical and environmentally friendly (1).

The majority of biotransformations occur in aqueous media, since the presence of organic solvents frequently hinders the activity of enzymes. However, solubility and stability of organic soluble substrates/products is often poor in an aqueous environment, and product yield and recovery is thus problematic. Two-phase systems may be appropriate for some whole cell bacteria or fungi, if a tolerance for organic solvents is observed. Examples of such systems are the decarboxylation of ferulic acid to 4-vinylguaiacol by *Bacillus pumilus* in an aqueous/hydrocarbon solvent system (2) (see Figure 6), the oxidation of cholesterol to cholestenone by *Arthrobacter simplex* in a

water/tetrachloride mixture (3), and the conversion of hydrocortisone to prednisolone by *Bacillus* and *Arthrobacter* sp. in an aqueous/organic solvent system (4) (see Figure 5). However, some cells, particularly mammalian cells, do not perform at all in this type of system since they are far more fragile than their bacterial/fungal counterparts. Microencapsulation may provide the protection these cells require and in addition, allow substrates/products to exist in an organic environment.

The objectives of this thesis were to obtain a system for the bioconversion of water insoluble substrates, using human kidney carcinoma and mouse liver mammalian cells, by formation of microcapsules via interfacial polymerization. In addition, the kinetic advantages/disadvantages between free cell, two-phase and encapsulated biotransformation of nitriles using *Rhodococcus rhodochrous* were explored.

1.0 Interfacial Polymerization

Microcapsules are small particles between 3 and 800 μm in diameter, which contain a core material surrounded by a coating or shell (5). Many methodologies have been adopted in formation of these capsules, all of which vary according to the substance being encapsulated and its application. One method, which was used in this thesis, is interfacial polymerization. This type of

microencapsulation was developed by Chang in Canada in the 1960's (6). Kondo and coworkers in Japan have also done extensive work in this area (5).

The capsule shell is formed at or on the surface of a droplet by polymerization of reactive monomers. Referring to Figure 1, the process involves the addition of an aqueous droplet, which contains the cells to be encapsulated along with one of the monomers, to an organic solvent, which contains a surfactant. This causes a stable emulsion to form whereupon polymerization is initiated by the addition of the second monomer in excess organic solvent. Rapid polymerization (10^2 - 10^6 dm³/mol.sec) at the interface upon contact of the two monomers occurs, generating the capsule membrane. The membrane produced is semi-permeable, allowing small molecules such as substrates and products to enter/exit and large molecules such as proteins and cells to remain within/outside the membrane (pore size ~ 2 nm) (5).

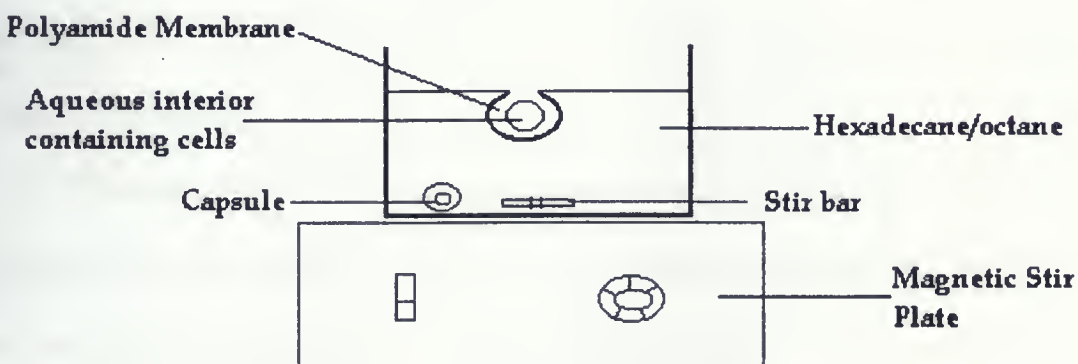


Figure 1: Methodology of Interfacial Polymerization

Different monomer-monomer combinations can be used to create various types of membranes, examples of which are given in Figure 2. Polymerization of terephthaloyl chloride with 1,6-hexane diamine produces a poly-(terephthalamide) membrane. Substituted diamines can be used to give the membrane a charged group, as in the case of L-lysine. Polyester microcapsules are formed by reacting sebacoyl chloride with 2,2-bis(4-hydroxyphenyl) propane. Polyurea and polyurethane membranes can also be made by the appropriate choice of monomers. The monomer combination chosen for the encapsulation process performed in this research uses a poly (allylamine) along with an extended chain diacid called dodecanedioyl chloride, which is more hydrophobic than sebacoyl chloride, producing a polyamide polymer.

Polyamide or nylon type membranes (Figure 2,(d)), have been used for encapsulation of yeast cells by Khan and coworkers for biotransformations in organic solvents (7). These capsules were found to be mechanically stable, resistant to organic solvents, and have high mass transfer rates of substrates/products.

The precipitation of the nylon polymer has been assumed to occur on the organic side of the interface. The formation of the membrane creates a barrier for the diffusion of the monomers and stops the polymerization reaction from continuing to completion, limiting the thickness of the membrane (5).

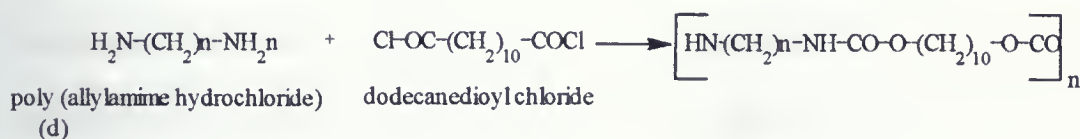
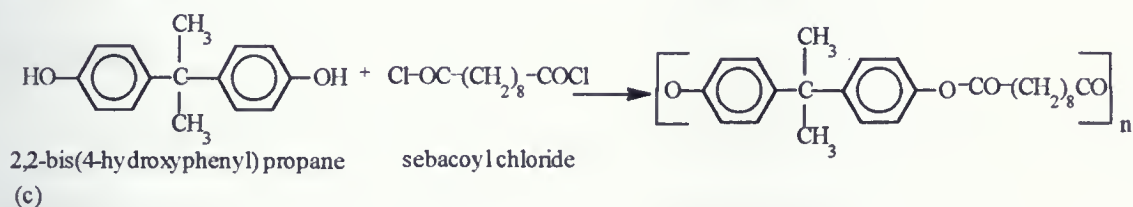
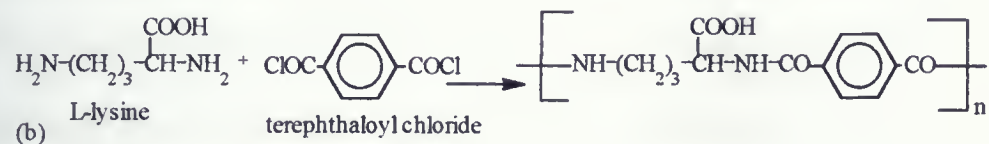
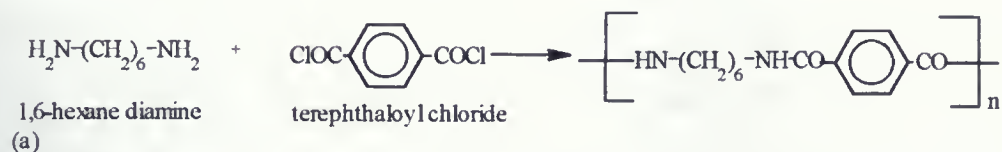


Figure 2: Monomers used for Interfacial Polymerization

(a) poly(terephthalamide), (b) poly(terephthaloyl L-lysine),
(c) polyester, (d) nylon

The partition coefficient of the polyamine dictates the levels of diamine at the reaction site. The rate of transfer to the active site must be greater than the rate of removal by polymerization to obtain a stable capsule (5). The concentration ratio of the two monomers is important for effective polymerization, however the amounts used are usually restricted by other conditions such as toxicity to the cells. Normally, one reactant is used in excess,

but for encapsulation of cells a 1:1 ratio is used to lower the amounts of unreacted monomers.

The stir rate dictates the size of microcapsules produced and also makes the difference between usable capsules and a useless mass of polymeric material (5). A faster stir rate produces smaller capsules, which, using a magnetic stirrer can be as small as 10-20 μm in diameter. When encapsulating cells, a slower stir rate is used to minimize shear stress and vortexing, which can damage cell membranes.

Solvent interactions with nylon membranes play a role in the thickness of the capsule produced. More polar solvents such as chloroform give thick films, whereas cyclohexane gives thin films. The density of the solvent affects the stability of the emulsion and determines whether the capsules sink or float in the organic phase, which in turn dictates the method of recovery for the capsules. Above all, solvents with a low toxicity to the cells are usually chosen (5).

Surfactants, which aid in formation of the emulsion, also play a role in the transfer of the polyamine to the organic phase. It was found with Span 85 (sorbitan trioleate) that increasing the amount of surfactant increases the amount of polyamine which reaches the organic phase (5). However, the main requirements of the surfactant is that it does not react with the acid chloride, contains no impurities which would interfere with polymerization, and is not toxic to the cells (5).

Interfacial polymerization reactions are conveniently performed at room temperature. No advantage exists for increasing the temperature, and lowering it to 4°C does not affect polymerization. Performing the reaction at 4°C is most advantageous for encapsulating cells and proteins since the stability of enzymes in solution is favourable at this temperature (5).

1.1 Applications of Encapsulated Systems

Khan *et al.* (7) developed a protocol for microencapsulation of yeast using interfacial polymerization and compared it to the conventional methods of cell immobilization using carrageenan and alginate beads. Multiple monomer pairs were tested for capsule formation to find a suitable combination for the desired conditions of biotransformation. Poly-(allylamines), poly (ethylene glycols), *O,O*-bis(2-aminopropyl)-poly (ethylene glycols) and poly(ethylene imines) were tested for their partitioning capacity between an aqueous buffer of pH 6-8 in the presence of Span 85 and octane. Poly(allylamine) mixtures were found to have the best partitioning, yielding capsules with good mechanical stability. In addition, larger polymers were thought to be less toxic to the cells (7). The microcapsules produced by interfacial polymerization were 50-300 μm in diameter. The encapsulated yeast cells were tested by biotransformation of 1-phenyl-1,2-propanedione in decane, as shown in Figure 3.

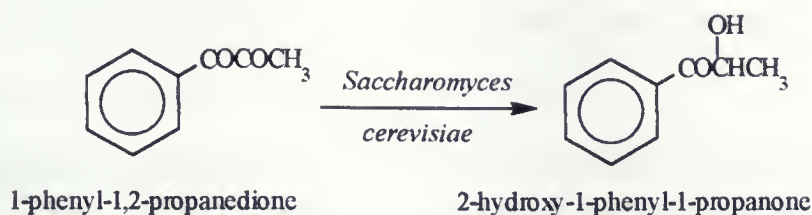


Figure 3: Biotransformation of 1-phenyl-1,2-propanedione

In the free cell bioconversion, yeast cells were rapidly inactivated, resulting in 7% yield of product. The encapsulated system allowed for 80% uptake of the substrate into the capsules and accumulation of product in the organic phase within 48 hr (7). The yeast cells survived longer due to the aqueous environment provided by the capsules and increased product formation resulted (7).

Alginate beads are made from the polysaccharide based sodium salt of alginic acid. Cells are suspended in a buffer solution and added to sodium alginate, stirred and added drop wise to CaCl_2 . The gel-like mixture solidifies in the calcium chloride solution upon ion interaction between the calcium and alginate ions. Carrageenan beads are similarly prepared by the addition of cells suspended in buffer to carrageenan. This solution is stirred and added drop wise to a solution of KCl to form beads. Carrageenan and alginate beads are larger in size (1-3 mm), and as a result, when compared with the polyamide capsules, the yeast biotransformation of 1-phenyl-1,2-propanedione was slower due to mass transfer limitations. In addition, polyamide capsules performed far

better in the presence of organic solvents than the other beads due to increased mechanical stability (7).

Alginate has been used by Chang and coworkers (8) to encapsulate and grow recombinant yeast cells, which overproduce an invertase enzyme that is excreted extracellularly. The encapsulated cells were kept in their aqueous growth medium for 24 hr and found to express more invertase activity than those in the free medium (8). The capsules could then be recycled and stored for up to one month, making downstream processing much more facile since the cells are easily separated, and isolation of the invertase enzyme is more rapid.

When encapsulating mammalian cells, the major application has been in the medical industry. Encapsulated cells have been used to treat a variety of human diseases such as hormone or protein deficiencies, by providing a method of cell delivery. Transplantation of cells has been limited because the cells are quickly destroyed by the recipient's immune system. Pancreatic islets (cells which produce insulin) have been encapsulated using many different methods in an attempt to make a capsule which will prevent the cells from being destroyed upon introduction to the recipient's body for treatment of diabetes.

Wang *et al.* (9) used capsules that were composed of a mixture of alginate and polymethylene-co-guanidine, prepared by precipitation with CaCl_2 and NaCl . These capsules are 0.5 mm to 3.0 mm in diameter with a membrane

thickness of 0.006 mm to 0.125 mm and have good permeability, which allows insulin to exit. Transplantation into mice showed a decrease in blood glucose levels for approximately 4-6 months (9). It is believed that malfunction of the capsules was due to the death of the islets themselves or to immune attack rather than capsule disruption.

Another polymer system used by Dawson and coworkers (10) for encapsulation of Chinese hamster ovary fibroblasts used an organic soluble hydroxyethyl methacrylate-methyl methacrylate copolymer (HEMA-MMA), prepared by interfacial polymerization. Droplets containing the polymer solution (73% HEMA-MMA in ethanol, 1% azo-bis-isobutyronitrile (AIBN)) along with the cells were extruded into phosphate buffered saline (PBS) containing surfactant, overlaid with hexadecane. The capsules were allowed to precipitate at the hexadecane/PBS interface for 30 min where AIBN initiated the polymerization. The capsules produced were ~1 mm in diameter, with a non-uniform shell being produced (10). The cells were able to endure the encapsulation process and survive up to 3 days, but viability was greatly reduced.

Recently, pancreatic islets (in tissue form) were encapsulated by silica sol-gel technology. Peterson *et al.* (11) developed a biocomposite material containing silica ceramic, prepared by polymerization in liquid solutions at room temperature and physiological pH. A two-step method, which involves

hydrolysis of a silicon alkoxide precursor under acidic conditions and gelation is induced through the addition of a base. Tetraethoxysilane (TEOS) was the polymer used. The gel is prepared before addition to the cells, which are added rapidly with stirring afterward. The mixture is then added drop wise to a beaker filled with vegetable oil and stirred for 30 sec, allowing capsules to form. The capsules had diameters between 200-1000 μm with corresponding surface areas of 996 m^2/g . The pore diameters were small (approx. 105 Angstroms), allowing IgG antibodies to be excluded, but still large enough to allow insulin to escape (11). The approach allowed the cells to survive up to 1 month *in vivo* following transplantation in mice. This technology has also been used for encapsulation of lipase enzymes by Reetz (12) for use in organic solvents on an industrial scale. Esterification reactions using traditional lipase powders forms a viscous enzyme- containing residue, which is difficult to recycle. In contrast, the lipase-containing gels are easy to separate and recycle (12).

Bacterial cells have been encapsulated by polyvinyl alcohol (PVA) membranes by Ariga *et al.* (13) and Bauer *et al.* (14). Ariga and coworkers prepared these capsules by mixing the polymer solution with the cells and dropping the suspension into cold methanol. The capsules were then washed in PBS to remove the excess methanol (13). The PVA capsules are for use in an aqueous environment, and do not allow leeching of the cells as some alginate and carrageenan beads do. It was found that with minimal exposure of the cells

to methanol, sufficient growth of the cells occurred at a much slower rate than in free solution, perhaps due to a diffusion limitation of oxygen (13).

PVA was also used by Bauer *et al.* (14) to encapsulate *Rhodococcus rhodochrous* in the conversion of propionitrile.

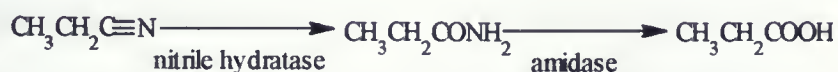


Figure 4: Biotransformation of propionitrile using *Rhodococcus* sp.

The biotransformation was performed in Na/K-phosphate buffer, pH 7 between temperatures of 40-60 °C. It was found that the PVA capsules were unstable at temperatures > 50 °C, but successful biotransformation over a broad pH range (pH 2-13) was successful. It was found with increasing concentration of propionitrile, increasing amounts of amide were produced but the amount of acid conversion remained constant throughout (14).

1.2 Two-phase Systems

The interest in undertaking biotransformations in low water environments has led to research involving aqueous/organic two phase systems. Layh and Willetts (15) explored the effects of organic solvents on the activity of nitrile hydratase from *Rhodococcus* sp. and nitrilase of *Pseudomonas* sp. (see Figure 4). The activities were measured by the total amount of products

formed from phenylacetonitrile in the presence of varying ratios of solvent to buffer. In the presence of nonpolar organic solvents such as iso-octane, octane, and hexadecane ($\log P > 4.0$), the activity of nitrile hydratase enzyme in cell free extracts from *Rhodococcus* sp. remained high in all ratios of solvent to buffer tested up to 75% (v/v). However, less hydrophobic solvents such as 1-octanol, and cyclohexanol caused significant loss of activity, even at 25% (v/v). The results were similar for the nitrilase extract from *Pseudomonas* sp. where full activity was retained at 50% (v/v) hexadecane (15).

Log P represents the log of the ratio of concentration of solute which partitions in the aqueous and organic layer respectively of a biphasic mixture (usually octanol/water) and is indicative of solvent polarity. Hence, a solvent with a high log P value (>4) is nonpolar and partitions poorly into the water phase. The results from Layh and Willetts (15) comply with the proposed generalization that biocatalysis is likely to be relatively high in the presence of solvents whose logP values are >4 , moderate with solvents of logP between 2-4, and low in hydrophilic solvents with logP <2 . Biotransformation using whole cells of *Rhodococcus* sp. and *Pseudomonas* sp. was also attempted in monophasic hexadecane and octane with no activity being detected, suggesting that the presence of some water was necessary for conversion (15). Most enzymes require an aqueous layer or shell on the outer surface to maintain stability and integrity. The ability of nitrile hydrolyzing enzymes from both *Rhodococcus* sp.



and *Pseudomonas* sp. to retain activity in organic/aqueous biphasic mixtures makes it possible to enhance biotransformation of water-insoluble nitriles.

Steroidal drug production by biocatalysis is also hindered by the poor solubility of substrates in reaction mixtures. Manosroi *et al.* (4) investigated free cell versus immobilized in aqueous and two-phase systems. The biotransformation of hydrocortisone to prednisolone by dehydrogenase enzymes in *Bacillus* sp. and *Arthrobacter* sp. is given in Figure 5.

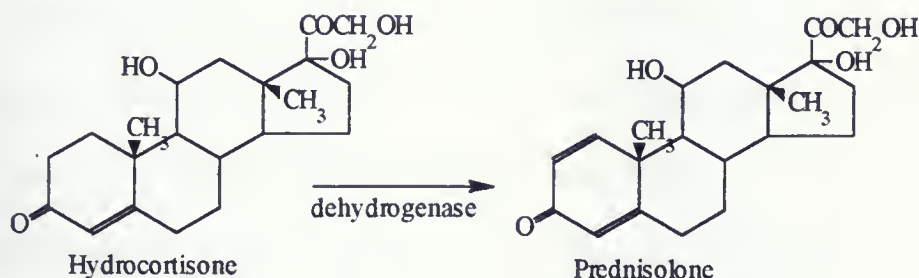


Figure 5: Biocatalysis of hydrocortisone to prednisolone

Hydrocortisone and prednisolone are both corticosteroids used as anti-inflammatory agents. The introduction of a double bond between C1 and C2 increases the anti-inflammatory potency by approximately four fold over hydrocortisone. Biotransformation using immobilized *Bacillus* sp. in an aqueous phase medium showed increased yields of prednisolone (5-15% higher) over the free cell form (4). *A. simplex* bacteria showed no difference between free cell and immobilized systems. Various two-phase systems were tested, with the optimal

ones being a 1:6 ratio of decane:aqueous medium and a 1:30 ratio of butyl acetate:aqueous medium, respectively. *Bacillus* sp. (both free and immobilized) did not show marked improvement in prednisolone yield with the two-phase systems, but *A. simplex* (both free and immobilized) gave higher yields in the biphasic mixtures (10-15% higher). Turnover of hydrocortisone was faster for all bacteria in the two-phase systems, reducing the reaction time required for optimal yields, especially in the 1:6 decane system (4). 1:30 butyl acetate gave higher yields of prednisolone but took much longer (144 hr. as opposed to 6 hr (4)). Overall, *A. simplex* free cell biotransformation in 1:6 decane:aqueous medium gave the highest yield in the least amount of time (84%, 6 hr) (4).

A second example of two-phase biotransformation is the decarboxylation of ferulic acid to 4-vinylguaiacol by *Bacillus pumilus* (2), as shown in Figure 6.

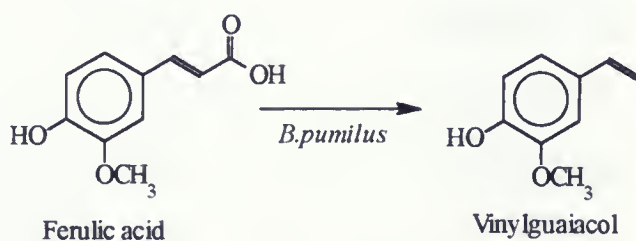


Figure 6: Conversion of Ferulic acid to 4-vinyl guaiacol

Ferulic acid is an abundant and renewable source of aromatic compounds from agricultural byproducts. Microbial transformations of ferulic acid to a wide

variety of aromatic compounds has been reported, with the most common being formation of vinylguaiacol (2). Vinylguaiacol is useful because it has been chemically transformed into more biodegradable, oxygenated polystyrenes which have increased durability over polystyrenes, and also into the flavour agent vanillin (2).

In an attempt to optimize vinylguaiacol yield, Lee *et al.* (2) used a two-phase system and whole cell *B. pumilus* bacteria. The ferulic acid decarboxylase enzyme has been isolated and found to require no cofactors or prosthetic groups, but whole cells provide protection against organic solvents during transformation. The carboxylic acid substrate is soluble in water, but the product is poorly soluble (1.7 g/L at 25 °C). In addition, ferulic acid decarboxylase is prone to substrate and product inhibition (2). This reaction is the ideal case for developing a two-phase aqueous/organic reaction system because the organic solvent permits the ready separation and recovery of lipophilic product from the hydrophilic substrate ferulic acid.

Various organic solvents were tested based on the partitioning of ferulic acid and vinylguaiacol between the organic and aqueous phase. Partition coefficients of ferulic acid were < 1 in all cases, and extremely low (< 0.01) with hydrocarbon solvents. The highest partition coefficients measured for vinylguaiacol were 167 and 120 in chloroform and ethyl acetate buffer systems. With hydrocarbon solvents, partition coefficients of vinylguaiacol were between

6-7. These results indicate that most of the vinylguaicol formed would transfer to the organic phase while ferulic acid would remain largely dissolved in the aqueous buffer, pH 6.8 (2). Ferulic acid decarboxylase activity was found to be three times higher in two-phase systems (0.4-0.5 $\mu\text{mol/min}$) than that obtained in buffer solution alone (0.16 $\mu\text{mol/min}$) (2). Hydrocarbon solvents showed the highest activities, suggesting that enzyme activity is stable in nonpolar environments. Based on partitioning behavior and reaction yields obtained, a hexane:phosphate buffer pH 6.8 two-phase system was selected. Different ratios of organic to aqueous media were tested, and the highest product yield was obtained with a 1:1 ratio (2).

As the concentration of ferulic acid was increased from 5-15g/L, vinylguaicol synthesis decreased, and leveled off at 40% conversion when ferulic acid concentrations exceeded 15 g/L. This result demonstrated that whole-cell ferulic acid decarboxylation is subject to substrate inhibition. To accommodate the problem of ferulic acid inhibition, a fedbatch operation was performed in which 5g/L ferulic acid was added intermittently to the ongoing reaction. Vinylguaicol production increased to 80% yield giving 7.6 g/L of product after 5 hr (2).

Based on the examples discussed, a two-phase system for the conversion of a water insoluble nitrile compound, 2-(4-chlorophenyl)-3-methylbutyronitrile (CPIN) by *Rhodococcus rhodochrous* was investigated for this thesis. CPIN is

transformed to an amide intermediate, which is potentially useful medicinally as an anti-inflammatory agent. The metabolic pathways involved in this bioconversion will be discussed in the next section.

1.3 *Rhodococcus rhodochrous* biotransformation of nitriles

Nitriles (cyano compounds) are important in synthetic organic chemistry, as precursors that can be transformed to amines, amides, carboxylic acids and other compounds. However, the major drawback of these compounds is that the hydrolysis to amides or carboxylic acids usually requires rather drastic conditions such as heating in the presence of strong acid or base (16-19). Referring to Figure 7, chemical hydrolysis of nitriles proceeds in two steps.

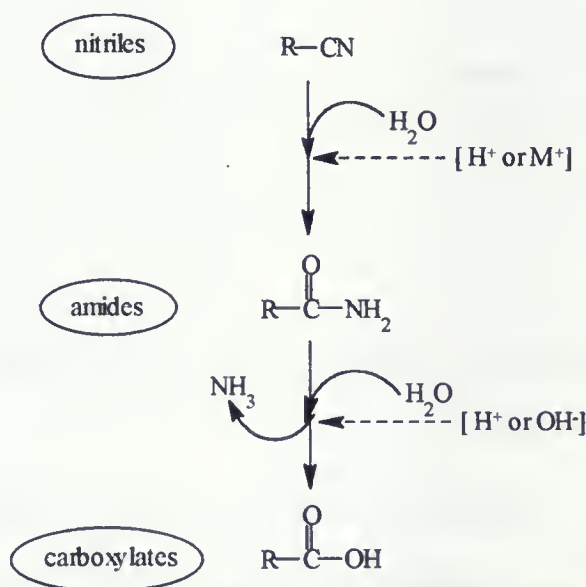


Figure 7: Chemical hydrolysis of nitriles (17)

Conversion to amides requires proton (H^+) and/or metal cationic species (M^+) which work to activate the carbon-nitrogen triple bond, facilitating the addition of water molecules (17). During the hydrolysis from amide to carboxylates, the C-N bonds are more resistant to cleavage by water molecules than conventional C-O bonds of esters, making harsh acidic or basic conditions required (17). This situation has made selectivity difficult, especially with molecules containing other acid/base sensitive functionalities.

Enzymatic or microbial transformation of nitriles is very attractive due to the mild reaction conditions it provides. Three enzymes, nitrile hydratase, amidase and nitrilase are known to convert nitriles to amides or carboxylic acids via two separate metabolic pathways, as shown in Figure 8.

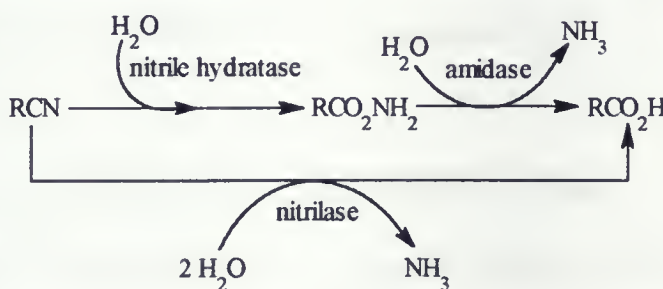


Figure 8: Enzymatic hydrolysis of nitriles (16-19)

A two step pathway converts nitriles to carboxylic acids via an amide intermediate. The nitrile hydratase enzyme creates an amide substrate, used by

a second enzyme, amidase which hydrolyzes it to a carboxylic acid and ammonia. Nitrilase enzymes hydrolyze nitriles to acids in one step (17).

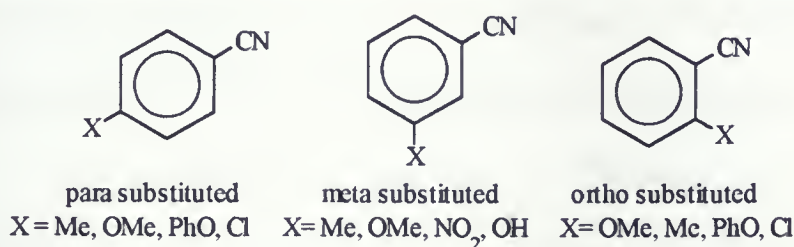
These enzymes are known to exist in some plants and fungi, but are more frequent in bacteria (20). Examples of nitrile degrading bacteria are *Pseudomonas* sp., *Nocardia* sp., *Corynebacterium* sp., and several strains of *Rhodococcus* sp.. Some bacteria utilize both pathways whereas others possess one or the other. Often, nitrile hydratase and nitrilase enzymes can be induced by addition of amide/nitrile containing compounds during growth but the physiological role of nitrile-degrading enzymes in bacteria is by no means clear. In plants, they are believed to be involved in a complex pathway for nutrient mobilization, particularly in the degradation of glucosinolates (20).

The bacterial strain used in this thesis, *Rhodococcus rhodochrous* ATCC 17895, converts nitrile compounds via the nitrile hydratase/amidase pathway. Hence, these enzymes will be discussed in more detail.

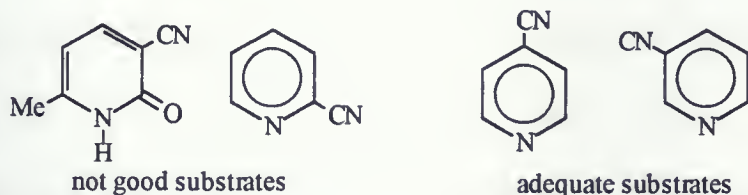
1.3.1 Substrate specificity of nitrile hydratase and amidases

The range of nitriles which are capable of being hydrolyzed by nitrile hydratase/amidase is broad. Referring to Figure 9a, benzonitriles with *para* substitution are accepted by microbial systems to give acids, while the isolated nitrile hydratase yields amide. *Meta*-substituted substrates are also converted to acids as well. *Ortho* substitution on benzonitriles leads to substrates which are

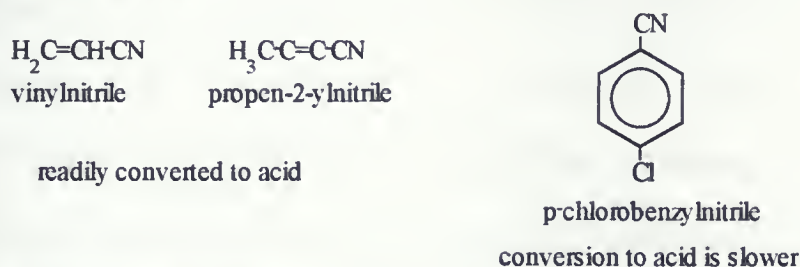
more sterically hindered, resulting in slower conversions to acid, with substantial amide production occurring. The amide to acid conversion is slower than the nitrile to amide step since steric hindrance has the most impact on the amidase enzyme (21). Heterocyclic nitriles (Figure 9b) are also converted by nitrile hydratase and amidases, but six membered heterocycles bearing a C=O or



a: Benzonitriles (21)



b: Heterocyclic nitriles (21)



c: aliphatic and benzonitriles (21)



d: dinitriles and diamides (17)

Figure 9: Substrate selectivity of nitrile hydratase and amidase

C=N group adjacent to the nitrile are poor substrates. These functionalities act like an *ortho* substituent, causing hindrance (21). The presence of an N-heteroatom or an amine substituent *para* to the nitrile results in low amide hydrolysis, perhaps due to competitive interaction of the nucleophilic nitrogen atom with the active site of the amidase (21). Aliphatic and benzonitriles (Figure 9c) are hydrolyzed to their corresponding acids with ease, but adjacent bulky groups can slow amidase-catalyzed conversion. Dinitriles (Figure 9d), yield monoamide and monoacids whether they are present on aliphatic or aromatic structures (21).

The stereoselectivities of nitrile hydratase and amidase enzymes are important, since they produce chirally pure products. Chiral molecules are those having the same molecular structure, but differing orientation in space, they are non-superimposable mirror images. When the two mirror image forms, or enantiomers, are present in equal amounts, the mixture is called racemic (22). The *R* and *S* nomenclature is used to distinguish the two forms, similar to amino acids in proteins which use L- α -amino acids (all of *S*-configuration, except for L-cysteine which is *R*). Enantiomers of chiral compounds interact with enzymes in different ways and can produce different physiological responses, which is why the pharmaceutical industry requires chirally pure drugs.

Ibuprofen is used as a nonsteroidal anti-inflammatory agent. The *in vitro* biological activity is known to reside with the *S* enantiomer. *Rhodococcus*

butanica hydrolyses α -arylpropionitriles such as **a** in Figure 10 with some chiral discrimination. The products are the corresponding *R*-amide **b** in 48% yield and 99% ee and the enantiomeric *S*-carboxylic acid, ibuprofen, **c** in 13% yield and 87% ee with the unreacted nitrile, **d** recovered in 73% ee (22).

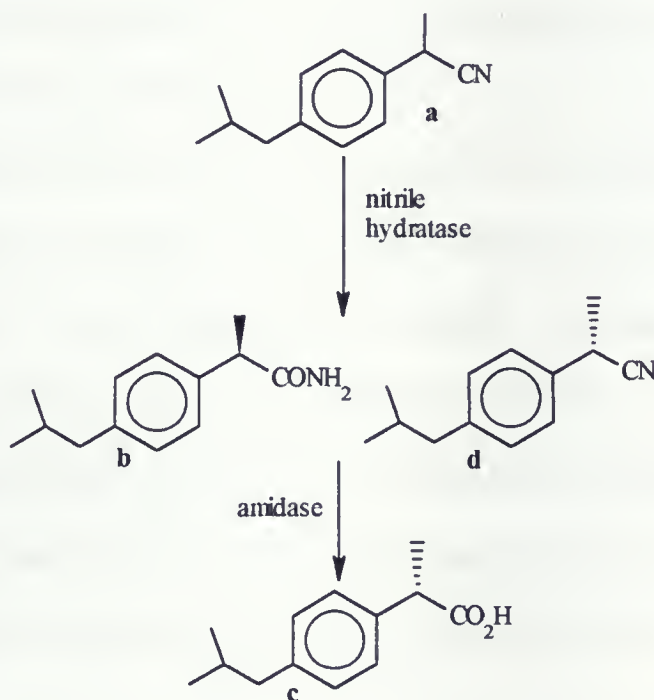


Figure 10: Biotransformation of nitrile, **a, by *Rhodococcus butanica* to give *S*-(+)-Ibuprofen, **c** (22)**

Rhodococcus butanica contains a stereospecific nitrile hydratase which prefers the *R* form of the nitrile, **a**, and a stereospecific amidase which prefers the *S* form of the amide intermediate. Another strain, *Rhodococcus* sp. AJ270 was used by Snell and Colby (23) for the same biotransformation to Ibuprofen, using the amide intermediate as the starting material. It was found that this strain

converted the amide to acid in 98% yield after 16hr, with both enantiomers being hydrolyzed. Significant ee values were only observed on partial hydrolysis, such as 94% ee at 35% conversion (23). These examples illustrate that the same biotransformation can be performed differently by various strains of the same bacteria. Hence, characterization of nitrile-metabolizing bacteria based on the biotransformations they perform is useful for prediction of the chiral products one can obtain from a particular strain.

2-Isopropyl-4-chlorophenylacetonitrile (CPIN), as mentioned previously, is the nitrile under investigation in this thesis. The amide product is useful as an anti-inflammatory agent, especially in its chirally pure form, and the acid product has some use as a pyrethroid insecticide, with the *S*-enantiomer having the greatest potency (24). Masutomo *et al.* (24) performed the biotransformation of CPIN using *Pseudomonas* sp. B21C9. Referring to Figure 11, stereoselectivity resided with the amidase enzyme and not the nitrile hydratase.

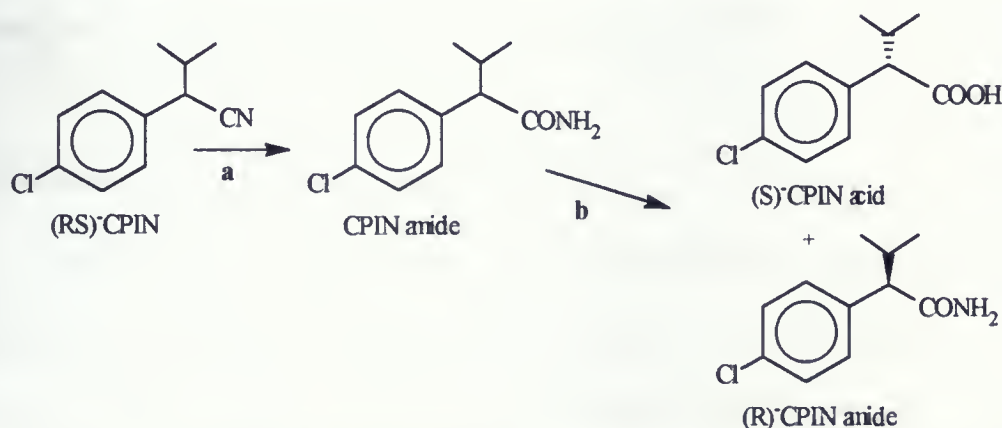


Figure 11: Scheme of hydrolysis of CPIN by *Pseudomonas* sp. B21C9
a: Nitrile hydratase having poor (*S*)-selectivity, b: amidase having strict (*S*)-selectivity (24)

A small amount of selectivity was shown by the nitrile hydratase enzyme early in the reaction, with the *S*-CPIN being hydrolyzed first, and subsequent hydrolysis of the *R*-CPIN enantiomer (24). The amidase appears to have strict *S*-selectivity, yielding optically pure CPIN acid with 100%ee and enantiomerically resolved *R*-CPIN amide with 100%ee (24). In addition, *R*-CPIN amide can be racemized by heating at 250 °C, which makes this biotransformation suitable for production of *S*-CPIN acid in higher yields (24).

Fallon *et al.* (25) performed CPIN biotransformation with *Pseudomonas putida* NRRL-18668 which contains a nitrile hydratase with high selectivity for *S*-CPIN. *R*-CPIN was also hydrolyzed at a much slower rate, but only after the *S*-enantiomer was gone, suggesting kinetic preference rather than absolute selectivity by nitrile hydratase (25). *S*-CPIN amide was obtained with 56%yield and 95% ee at 30 °C. The CPIN amide was not a substrate for the amidase since CPIN acid was not detected. Stereoselectivity usually resides exclusively with the amidase enzyme, making this case a rare example (25).

1.3.2 Enzymatic Mechanisms of nitrile hydratase

Bacterial nitrile hydratases are structurally similar, consisting of α and β subunits, with high levels of sequence homology in the β subunit and not the α subunit. X-ray crystallographic structures revealed that the N-terminus of the β subunit is conserved and buried in the center of the $\alpha\beta$ heterodimeric interface.

The N-terminus of the α subunit was not buried, but is still involved in dimer stabilization by wrapping across the surface of the β subunit (20). The quaternary structures of nitrile hydratases are highly variable, ranging from 30-505 KDa. Most nitrile hydratases are $\alpha\beta$ heteromultimers, typically dimers or tetramers, with α subunits between 24-28 KDa and β subunits of 25-39 KDa (20).

Nitrile hydratases contain Fe^{3+} or Co^{3+} centers within the α subunit. *Rhodococcus* R312 nitrile hydratase binds two Fe atoms using 3 cysteine thiolates and two main chain amide N atoms as ligands. Referring to Figure 12, some non-heme Fe-containing nitrile hydratases of *Rhodococcus* sp. show an interesting photoactivation effect.

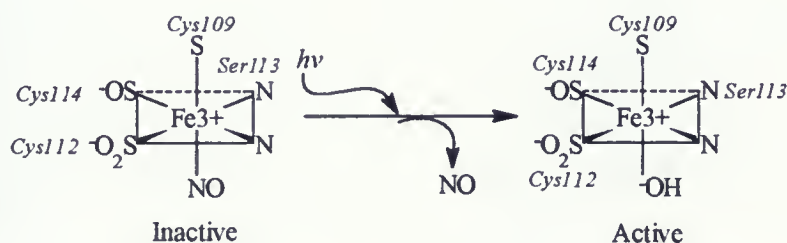


Figure 12: Possible scheme for NO-dependent activity regulation of the photoreactive *Rhodococcus* sp. nitrile hydratase (26).

The five iron ligands have an octahedral arrangement, with the sixth position being unoccupied. Cys112 and Cys114 are post-translationally oxidized to cysteine-sulfinic and sulfenic acid respectively (26). In the active form, a hydroxide ion is believed to occupy the sixth position, with an endogenous NO

being bound in the inactive form. The inactive form prevails in the dark, with light irradiation transforming it to the active form by release of NO, causing a conformational change in the enzyme (26). The oxidation of Fe^{2+} (which may bind NO) to Fe^{3+} upon release of NO could play a role in this photoactivation.

The exact mechanism of nitrile hydratases has not been elucidated, but two prevalent theories reside. Referring to Figure 13 (26), mechanism A illustrates the nitrile substrate approaching a metal-bound hydroxide ion, which can act as a nucleophile attacking on the nitrile carbon atom. Mechanism B shows a metal-bound hydroxide ion as a general base activating a water molecule which in turn attacks the nitrile carbon (26).

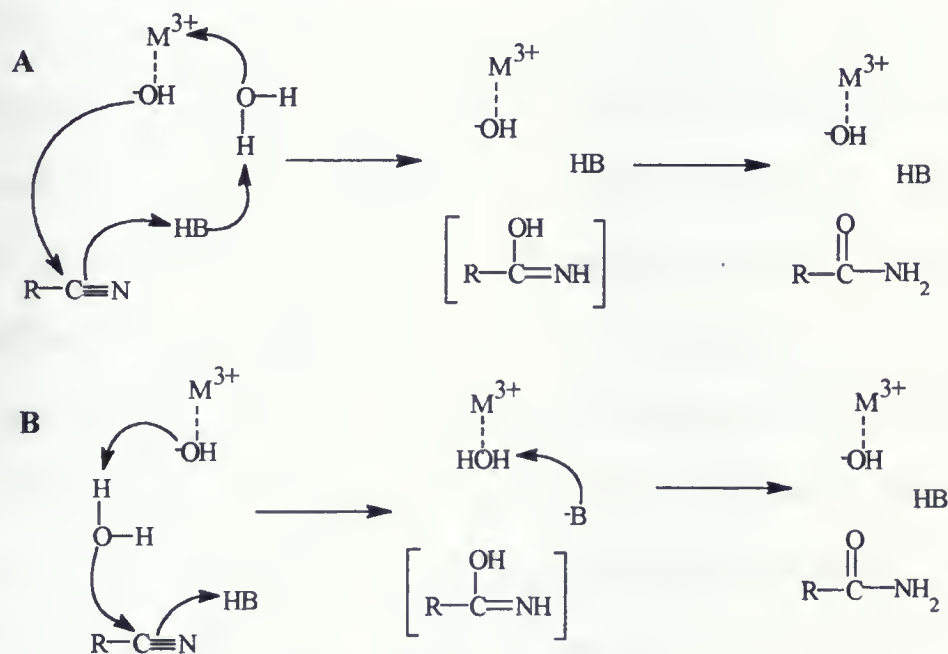


Figure 13: Postulated mechanisms of nitrile hydratase
 M: Iron or Cobalt, B: basic group of the enzyme (26)

The catalytic mechanism for Fe-containing nitrile hydratases is suggested to involve the Fe^{3+} center as a Lewis acid, either directly or indirectly activating the nitrile for hydration (20). Mechanisms involving the direct coordination of the nitrile N atom with the metal ion or attack by an Fe-coordinated hydroxyl group are thought to be unlikely since trivalent metal ions show slow rates of ligand exchange. Indirect attack via a water molecule, as in Figure 13 B, does not require ligand exchange and is consistent with the role of Fe^{3+} as a Lewis acid (20).

1.3.3 Mechanism of amidases

The amidase of *Rhodococcus rhodochrous* J1 has been sequenced, but its three dimensional structure is still under investigation. This amidase is thought to be membrane-bound, and involved in the process of inactivation of fatty acid amides, which act as neurotransmitters. In addition, amidases play a role in the biosynthesis of indoleacetic acid as an important hormone in plants, which lead to the discovery of how callus tissues are converted to individual plants (27).

Kobayashi *et al.* (27) performed a series of site-directed mutagenesis studies on *Rhodococcus rhodochrous* J1 amidase in order to elucidate important amino acid residues involved in amidase activity. Upon comparison of the amidase amino acid sequence with other amide metabolizing enzymes, four amino acids were found to be conserved. Mutants were created by replacing

Cys203 with Ala, Asp191 with Asn, Ser195 with Ala and Asp191 with Glu. Each mutant was tested for amidase activity, with zero activity detected for the Ser195 mutant and the Asp191 mutant (27). It was determined that Ser195 and Asp191 were essential for amidase activity, and although Cys203 was not essential, it was found to enhance enzyme activity (27).

Amidases are believed to operate by an acyl-enzyme mechanism (27,28). Kobayashi *et al.* speculated that the Asp191 of the *Rhodococcus* sp. amidase may function as a general base, abstracting the proton from the Ser195 hydroxyl sidechain, allowing the serine to act as a nucleophile for the carbonyl group of the amide bond within the substrate (27). Further research by Kobayashi *et al.* (28), lead to the proposed mechanism shown in Figure 14.

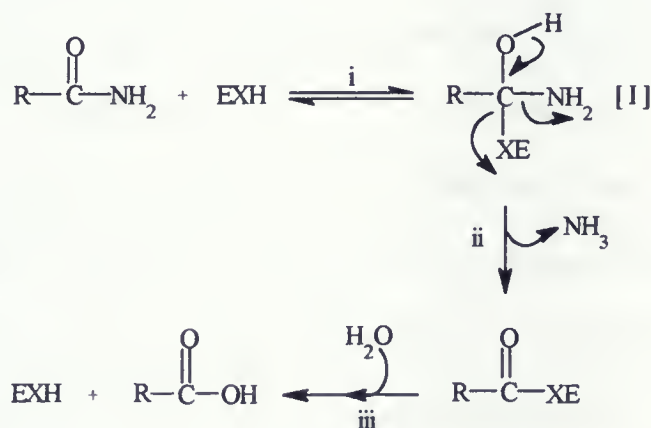


Figure 14: Proposed mechanism for the amidase reaction.

EXH: nucleophilic amino acid, [I]: tetrahedral intermediate (28)

The carbonyl group of the amide substrate is believed to undergo attack by a nucleophilic amino acid of amidase (possibly Ser195) represented as EXH in Figure 14, resulting in a tetrahedral intermediate [I] (28). This step i is reversible. After removal of ammonium (step ii), the tetrahedral intermediate is converted to an acyl enzyme, which is subsequently hydrolyzed to an acid (step iii) (28). Step iii cannot be reversible after step ii has occurred since the ammonium salt of benzoic acid was not converted to the amide in experimentation (28). Further studies on the three-dimensional structures of amidases would provide more clues as to the active site and mechanism of catalysis.

1.4 Mammalian Cell Metabolism

In this thesis, cultivation of mammalian cells was performed for encapsulation and biotransformation of pharmaceutical substrates. The products, or metabolites produced are transformed primarily by Cyt-P450 enzymes. Within mammalian cells, Cyt-P450 is found in the endoplasmic reticulum and the cytosol. These are the sites of phase I (functionalization reactions) and phase II (conjugation reactions) metabolism.

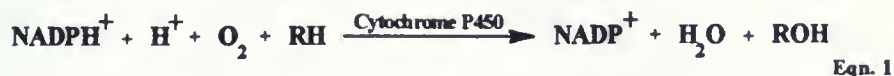
Phase I metabolism performs preparative steps for entry into phase II metabolism by uncovering or producing chemically reactive groups upon which phase II reactions occur. Phase I reactions usually convert the drug to a more

oxidized form, thus making it readily excretable. Phase II metabolism consists of true detoxification pathways and gives products that account for inactive, excreted products of a drug. Common reactions associated with metabolism are listed in Table 1.

Table 1: Reactions classed as phase I or phase II metabolism

Phase I	Phase II
Oxidation	Glucuronidation
Reduction	Sulfation
Hydrolysis	Methylation
Hydration	Acetylation
Dethioacetylation	Amino acid conjugation
Isomerization	Glutathione conjugation
	Fatty acid conjugation
	Condensation

During *in vitro* drug bioconversion, phase I metabolism predominates, which includes such reactions as oxidation, reduction, hydrolysis, hydration and other rarer reactions. The major reactions of most of these pathways occur via the mixed-function oxidase system (MFO). This enzyme system catalyzes the hydroxylation for hundreds of structurally diverse drugs and chemicals. All of these reactions require the presence of molecular oxygen and NADPH (enzymatic cofactor) as well as Cyt-P450, and all involve the transfer of one oxygen atom to the drug molecule (29). A subsequent rearrangement and/or decomposition of the product may occur, leading to the final metabolites seen. The mixed-function oxidase system conforms to the following equation:



where RH represents the drug to be oxidized and ROH the hydroxylated metabolite. During the MFO reaction, reducing equivalents derived from NADPH, and H^+ are consumed and one atom of molecular oxygen is incorporated into the substrate, whereas the other oxygen atom is reduced to water (29).

Three major elements compose the MFO system: those being Cyt P450, NADPH-cyt-P450 reductase, and lipids. Cyt-P450 is the final oxidase component of the electron transfer system and is responsible for many drug oxidation reactions. It is a heme-containing enzyme with an iron protoporphyrin ring (Figure 15) (29). The enzyme consists of a family of closely related isoenzymes embedded in the membrane of the endoplasmic reticulum and exists in multiple forms. It is responsible for binding both the oxygen and substrate in the MFO reaction.

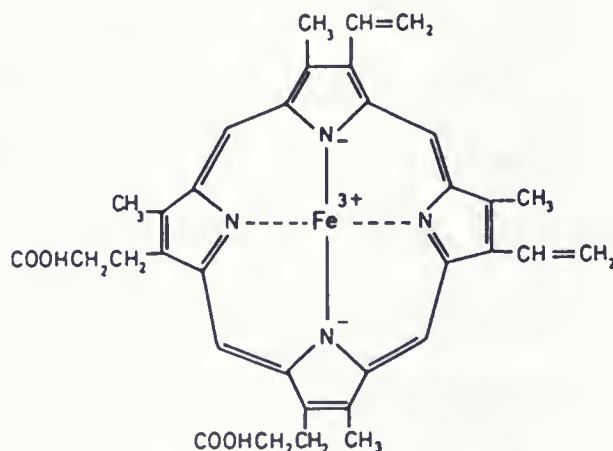


Figure 15: Cyt-P450 Protoporphyrin IX (29)

NADPH-cyt-P450 reductase exists in close association with Cyt-P450 and is involved in transferring reducing equivalents from NADPH to Cyt-P450 as such:

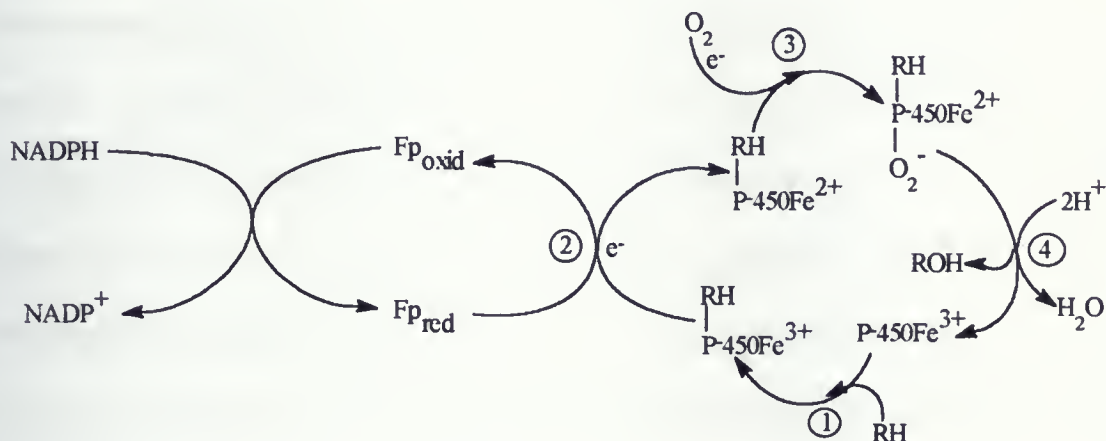


Figure 16: Cyt-P450 cycle in drug oxidations

RH: parent drug, ROH: oxidized metabolite, Fp: flavoprotein, e⁻: electron (30)

Oxidized (Fe³⁺) Cyt-P450 combines with the drug substrate (RH) to form a binary complex (step 1). NADPH donates an electron to the flavoprotein reductase which in turn reduces the oxidized Cyt-P450-drug complex (step 2). A second electron is introduced from NADPH via the same flavoprotein reductase, which serves to reduce molecular oxygen and to form an "activated oxygen"-Cyt-P450-substrate complex (step 3). This complex in turn transfers activated oxygen to the drug substrate to form the oxidized product (step 4) (30).

It has been shown that a heat stable lipid component is required by the MFO system during oxidation. The precise mode of action of lipids is still unknown but it has been suggested that lipid may be required for substrate

binding, facilitation of electron transfer or providing a template for the interaction of Cyt-P450 and NADPH-Cyt-P450 reductase (29).

In this thesis spironolactone, a steroidal drug used as a diuretic, was metabolized by human kidney carcinoma cells. Common biotransformations of steroids are ring hydroxylation and oxidative aromatization among other conversions. An example of hydroxylation is conversion of androst-4-ene-3,17-dione, a precursor of testosterone, which is hydroxylated in the 6β , 7α and 16α positions preferentially (Figure 17). This is an endogenous reaction of the MFO system, but the same enzymes also metabolize other steroid drugs, which can be hydroxylated in various positions (29).

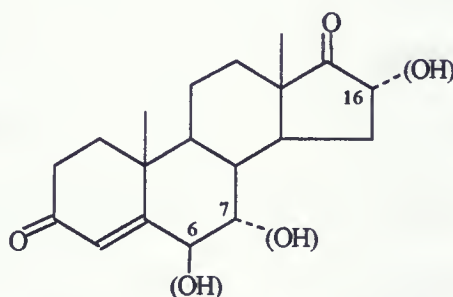


Figure 17: The hydroxylation of androst-4-ene-3,17-dione (29)

Oxidative aromatization of steroids by Cyt-P450 isozymes is common, as in the case of the anti-fertility drug, norgestrel. The A ring of norgestrel is converted to a phenol, as shown in Figure 18 (31).

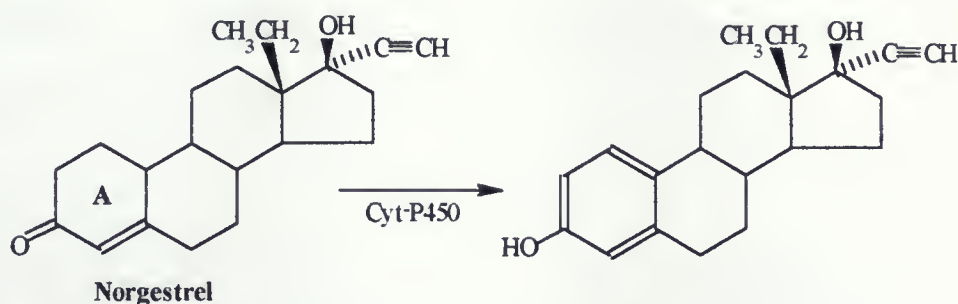


Figure 18: Metabolism of Norgestrel by Cyt-P450 (31)

Certain endogenous reduction reactions of steroids have been observed, but the relationship of these reactions to reduction of drug substrates is unclear (29).

Functional groups present in drug molecules such as secondary and tertiary amines, thiols, alkoxy groups and esters are prone to reactions such as dealkylation, N, S and C oxidation, methylation and hydrolysis. Hydrolysis is predominant for ester groups whereas oxidative reactions occur on heteroatoms or functionalities containing N, S and C atoms. An example of this is the S-oxidation of the anti-psychotic drug thioridazine. Referring to Figure 19A (29), both sulfur atoms are metabolized to the corresponding sulfoxides. The metabolite with only the methylthio substituent converted to the sulfoxide is twice as potent as an anti-psychotic drug (mesoridazine) (29). Another example of metabolism is the N-demethylation of a common tranquilizer, diazepam (Figure 19B) which is converted to N-desmethyldiazepam with the loss of methanal. The reaction is considered to occur in two steps, the first being

hydroxylation of the methyl group on the nitrogen, and the second a decomposition of this intermediate (29).

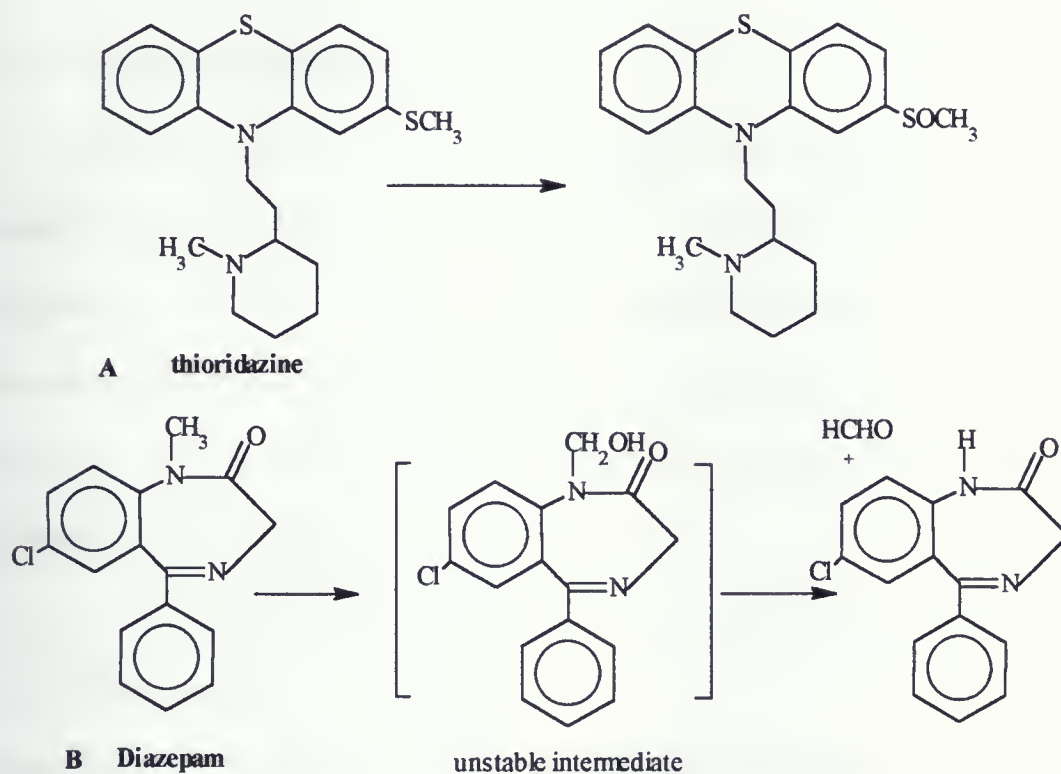


Figure 19:A; S-oxidation of thioridazine, B; N-demethylation of Diazepam (29)

Chapter 2: Experimental

2.1 Mammalian Cell Culture Project

All media and media components along with trypsin enzyme were supplied by Gibco laboratories. All cells were incubated in a Fisher scientific automatic CO₂ water-jacketed incubator and subcultured/manipulated in a Labcono purifier biological safety cabinet (laminar flow hood). In addition, all techniques used in cell maintenance and experimentation were performed aseptically using standard cell culture protocol.

2.1.1 Cell Cultivation

Mouse Liver Cells (MLC): This semi-anchorage-dependent cell line was obtained from American Type Culture Collection (ATCC) as CCL-9.1 NCTC clone 1469 derivative. MLC were routinely grown in 150x20 mm sterile tissue culture dishes with 28 ml of medium. The cells were grown in Dulbecco's modified eagle's medium (DMEM) supplemented with 10% (v/v) horse serum, 1% (v/v) L-glutamate and 1% (v/v) penicillin-streptomycin and kept in a controlled atmosphere of 5% CO₂ at 37 °C.

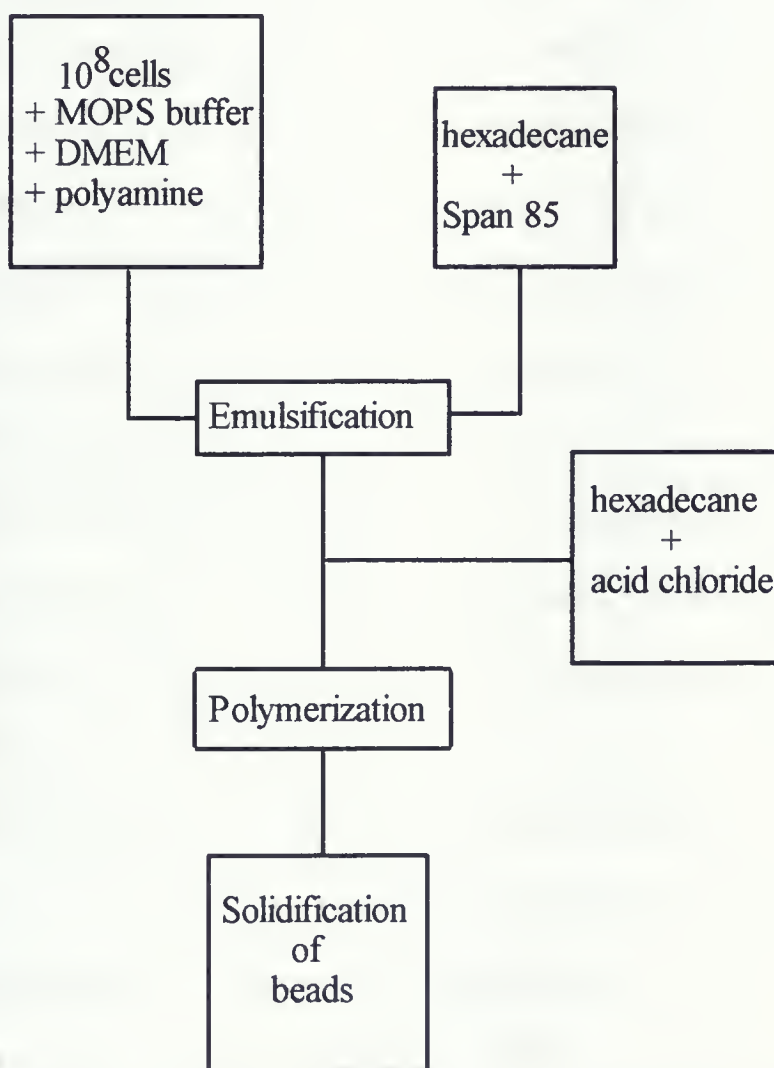
Cells were recovered by harvesting the medium, washing the petri dishes with phosphate buffered saline (PBS) (PBS washings were also harvested) and adding 1-2ml trypsin enzyme to the plates for approximately 1-2min upon which an incubation time of 20 min was allotted. The cells were passaged and transferred to sterile 50 ml polystyrene centrifuge tubes and centrifuged for 10 min at 1200 rpm. The supernatant was removed and the pellet resuspended in the appropriate amount of medium.

Human Kidney Carcinoma Cells (HKC): This adherent cell line was obtained from ATCC as CCL-13, A-498 Chang cells. HKC were routinely grown in 10% (v/v) Eagle's minimum essential medium (EMEM) supplemented with 8% (v/v) fetal (or donor) bovine serum (FBS), 1% (v/v) sodium pyruvate, 2.93% (v/v) NaHCO_3 , 1% (v/v) non-essential amino acids, 1% (v/v) L-glutamate and 1% (v/v) streptomycin -penicillin and kept in a controlled atmosphere of 5% CO_2 at 37°C.

Cells were recovered by removing the medium, washing petri dishes with PBS and adding 1-2 ml trypsin solution for 1min. Thereafter, the plates were incubated at 37°C for 15-20min. The cells were then passaged and resuspended in the appropriate amount of medium (1:4, 1:8 ratio of cells to medium for expansion).

2.1.2 Encapsulation Methodology

Encapsulation methodology was taken from J.A. Khan *et al.* (7). The concentrations of each chemical/buffer/polymer utilized were optimized for mammalian cell encapsulation conditions by performing toxicity assays and experiments as described in section 2.1.7.



Scheme 1: Flow chart for interfacial polymerization using PAA/acid chloride

Method 1: Encapsulation of mammalian cells (scheme 1): Mouse liver cells (10^8 cells, 0.5 ml packed volume) were added to 2 ml of a mixed solution containing 0.28 M 4-morpholinepropanesulfonic acid (MOPS) buffer, pH 7.8 and 0.076 M poly(allylamine hydrochloride) (PAA) in DMEM (DMEM was supplemented with 4% (v/v) glutamate). The suspended cells were placed on ice until their addition to hexadecane. A flat bottom 50 ml beaker containing a smooth 2.5 cm magnetic stir bar was filled with 20 ml of dry hexadecane and placed in a bath of cool water (cannot place on ice since hexadecane will begin to crystallize due to its low melting point). The apparatus was placed on a magnetic stir plate where 300 μ l of sorbitan trioleate (Span 85) was added to the hexadecane and allowed to mix. Dry hexadecane (15 ml) and 17 μ l of dodecanedioyl chloride were added to a 60 ml separatory funnel fitted with a septum to which was inserted a syringe filled with calcium chloride to act as a drying tube. The separatory funnel was clamped 5-6 cm above the hexadecane level in the 50 ml beaker. Stirring was adjusted to a slow rate in order to minimize vortexing and to reduce the shear stress.

The cell suspension was then added to the beaker using a sterile Pasteur pipette over a 5 min period. At this point, a sample was taken and viewed under a light microscope to observe pre-capsular stages (i.e. droplet size and concentration of cells within the droplets). The acid chloride/hexadecane mixture in the separatory funnel was added at this stage over 15 min while stirring. After addition was complete, the capsules were stirred for an

additional 30 min to allow for hardening of the interfacial membrane. If aggregation of capsules was observed, the stir rate was increased slightly.

Method 2: Encapsulation of substrate: This technique is known as reverse capsule formation since the aqueous phase is on the exterior of the capsule. MOPS buffer (40 ml, 0.6 M), pH 7.8 (saturated with hexadecane) was placed in a flat bottom 250 ml beaker under an overhead stirrer. While stirring at high speed (as high as possible without causing froth formation, approx. 1500 rpm), 10 ml dry hexadecane mixed with 800 μ l dodecanedioyl dichloride was added drop wise over 30 sec using a graduated pipette. The mixture was emulsified for 1 min. Subsequently, 25 ml of 0.12 M PAA (in 0.6 M MOPS, pH 7.8) and 2.5 ml 1 M PAA were added over 3 min and mixed for an additional 3 min. The mixture was placed on a magnetic stir plate and stirred at a lower speed for 1 hr to allow the capsules to cure. A small amount (1-2 ml) of 0.01% SDS was added to the capsules during the curing process to prevent aggregation. The formed capsules were washed and resuspended in MOPS buffer. Amine-containing substrates cannot be added during the encapsulation process since they will interfere with polymerization. Hence, they were added to MOPS buffer which contained the formed capsules and stirred overnight, whereupon the substrate diffused into the capsules. Other non-amine containing substrates were added during encapsulation along with the PAA solution.

Method 3: Encapsulation of substrate using dialysis tubing: Dialysis tubing was cut into 7 cm strips and boiled in distilled water for 30 min to remove debris and denature any proteins which may be present. The tubing was rinsed 3-4 times with distilled water and stored in the refrigerator until further use. One end of the dialysis strip was tied off with string (double knotted) and subsequently, the strip was autoclaved for 15 min in distilled water. To prepare a filled dialysis tube aseptically, disposable gloves, string, metal scissors, tweezers and Pasteur pipettes were autoclaved prior to use. The substrate was dissolved in 4-5 ml of the desired solvent (toluene, hexadecane) and added to the tubing (each holds 1-1.5 ml) with a Pasteur pipette, while wearing sterile gloves. The remaining end was tied off with sterile string. The filled tubes were then rinsed with sterile water and added to the Celligen bioreactor via one of the plug ports on the head plate. (All manipulations were performed in a laminar flow hood).

2.1.3 Viability Studies

Three methods for determining viability of the cells within the capsules were attempted:

Capsule disruption: Capsules were washed twice with saturated hexadecane (saturated with MOPS buffer), decanting each time. A third washing with 0.01% SDS in PBS was performed and a cellular sieve was used for harvesting of the capsules (which float in SDS solution). The cells were then rinsed with DMEM

medium and resuspended in fresh DMEM in a sterile 10 ml centrifuge tube. The capsules were then sonicated for 2.5-3 min and the mixture (capsular debris and cells) was seeded onto a petri dish, incubated and observed for viable cells the subsequent day. In addition, an aliquot of the cells was stained with Trypan Blue and viewed under a light microscope.

Viability via biotransformation: The washed cell-containing capsules were resuspended in 25 ml saturated hexadecane in a 250ml Erlenmeyer flask to which the substrate, pyrillamine maleate (prepared from the maleate salt as described later on) was added in a concentration of 3 mg/ml. The flask was capped with a foam plug and placed in a shaker incubator at 37 °C and 100 rpm. Biotransformation was halted after 4 days and the capsules were disrupted by sonication. Both the hexadecane and aqueous capsule layer were analyzed by Thin Layer Chromatography (TLC) for product formation.

Viability Staining: Cells were harvested at various intervals before, during and after capsule formation and these samples were stained using LIVE/DEAD viability/cytotoxicity kit (L-3224) purchased from Molecular Probes, Inc. The kit contains two components: calceinAM and ethidium homodimer (EthD-1). Hydrolysis of calceinAM is catalyzed by ubiquitous intracellular esterases which convert non-fluorescent cell-permeant calceinAM to the intensely fluorescent calcein. The polyanionic calcein is well retained within living cells producing an intense uniform green fluorescence. EthD-1 enters cells with damaged

membranes and undergoes a 40-fold enhancement of fluorescence upon binding to nucleic acids, thereby producing a bright red fluorescence in dead cells. EthD-1 is excluded by the intact plasma membrane of live cells. Hence, live cells fluoresce green where dead cells fluoresce red.

Optimal dye concentrations were determined by preparing samples of live and dead cells on microscope slides (cells were killed by treatment with 70% methanol for 30 min). Using the samples of dead cells, concentrations of 4,2,1 and 0.5 μM EthD-1 were added to the slides and examined for fluorescent intensity. The concentration at which the dead cell nuclei were stained bright red without staining the cytoplasm significantly was chosen to be 2 μM .

Using the samples of live cells and dead cells, concentrations of 4,2,1 and 0.5 μM calceinAM were added to the slides and examined for fluorescent intensity. The concentration at which sufficient fluorescence signals in live cells was shown without giving significant staining in the dead cells was determined to be 1 μM .

For examining samples before, during and after encapsulation, 0.5-1.5 μl aliquots were taken and suspended in 500 μl of dye solution (2 μM EthD-1, 1 μM calceinAM in PBS) whereupon 95 μl of this suspension was added to a microscope slide and allowed to incubate at 37 $^{\circ}\text{C}$ for 30 min. Slides were viewed under a fluorescent microscope where the number of viable cells per field of view was counted (an average of 10 fields of view was taken). Knowing the area

of the field of view (7.068 mm^2) and the area of the coverslip (484 mm^2), the total number of viable cells on the coverslip was calculated (68.47 fields of view/coverslip). Hence, the total number of viable cells/ml was determined. The viability of the cells was expressed as a percentage:

$$\% \text{ viability} = \frac{\text{number of viable cells}}{\text{total amt. cells}} \times 100\%$$

The total amount of cells/ml was determined by diluting a $5 \mu\text{l}$ sample of the cells immediately after harvesting, in 10 ml $\text{Ca}^{2+}/\text{Mg}^{2+}$ free PBS and placing $8 \mu\text{l}$ onto a haemocytometer. The haemocytometer contains a grid-marked counting chamber with known dimensions and volume. The number of cells/ml is determined by the following equation:

$$\frac{\text{\#cells in 5 squares}}{5} \times 10^4 \text{ml} \times \text{dilution factor}$$

2.1.4 Bioreactor

The bioreactor utilized for cell cultivation/biotransformation was the New Brunswick Scientific Celligen (Cell Culture System, 1.5 L model) purchased from New Brunswick Scientific Co. Inc. A steam sterilizable galvanic oxygen electrode (DO probe) was also purchased from the above named. An Ingold Combination pH electrode was purchased from Ingold Inc.

The Celligen has three major components; a 1.5L Pyrex glass vessel, a head plate containing various components, and a console from which culture conditions are controlled (see Figure 20). The head plate accommodates a cell lift impeller responsible for sparging the medium upon agitation. It does so in a manner that causes an influx of medium up through the shaft where gas exchange occurs and an efflux of medium through the port of the impeller. Air, oxygen, nitrogen, and carbon dioxide tanks are connected to the Celligen console

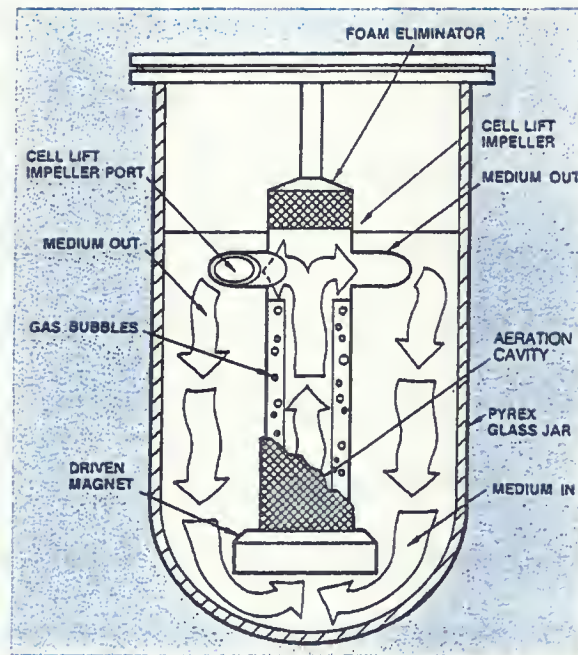


Figure 20: Schematic of Celligen

and gases delivered to the impeller in controlled amounts. The impeller itself is covered with a stainless steel mesh sleeve which reduces shearing of the cells and prevents any gas bubbles from entering the free medium. A stainless steel mesh surrounds the top of the impeller and acts as a foam eliminator. A platinum resistance temperature detector (RTD) present within the bioreactor measures the temperature of the vessel and this is indicated on a digital display within the console. A mat heater located within the vessel mounting clamp is responsible for heating the medium while a stainless steel condenser cools the system. A temperature is set on the console, and the RTD regulates the heating system around the set point. In addition, a galvanic pH electrode and dissolved oxygen probe report pH and oxygen content of the medium (also digital display). The reactor also has an exhaust system to which is attached an exhaust gas filter to maintain sterility. There are also addition and harvest tubes located in ports on the head plate which are responsible for adding and removing cells/medium. A sample tube attached to a sample vial is an additional component on the head plate which allows for sampling without the necessity of disassembling the Celligen. It is also important to mention that all attachment sites and outlets are sealed with O-rings to insure an airtight, low contamination environment within the bioreactor.

Assembly to Inoculation: All Celligen components were washed thoroughly with laboratory glassware soap and rinsed repeatedly with distilled water before assembly.

Step1: The impeller was assembled first due to its multiple parts and the fact that it must be added to the head plate where the agitation is tested before complete assembly of the Celligen. O-rings were placed strategically along the impeller shaft before and after every point of component attachment. The stainless steel mesh sleeve was added to the shaft, along with a driven magnet which again, is held in place with O-rings. The foam eliminator was attached to the top of the impeller shaft where it is then attached to the head plate via a shaft housing.

Step 2: The Pyrex vessel was filled with 1.2 L $\text{Ca}^{2+}/\text{Mg}^{2+}$ free PBS whereupon the impeller/head plate assembly was attached. The unit was placed on the console and held in place with the mounting clamp. The agitation was then turned on and the impeller was observed for irregular stirring at all rpm rates (50-230 rpm).

Step 3: The pH electrode was examined for low levels of electrolyte and filled if necessary. It was then attached to the console and calibrated using standard buffer solutions of known pH. Once calibrated, the fill ports on the electrode were plugged and inserted into the Celligen via the proper port on the head plate.

Step 4: The DO probe was examined for membrane integrity and electrolyte level and prepared appropriately. It was then attached to the Celligen.

Step 5: All other components such as the harvest tube, condenser, and sampler were added to the head plate which was attached to the vessel and sealed with a large O-ring.

Step 6: Glass adapters (male and female) were attached to the harvest and addition tubes via silicon tubing. In addition, vacant ports had plugs placed within and silicon tubing was used to seal off additional tube ports (glass wool was inserted in the ends which were then clamped off).

Step 7: Sterile filters were placed on the gas import and gas exhaust ports as well as on the sampler; clamps were placed at various points on the tubing pieces to provide an additional seal from the external environment. The reactor was checked for any openings which may have been forgotten and was prepared for sterilization.

Step 8: The apparatus was given a point from which pressure can be released during autoclaving by loosening the clamps which seal off the tubing attachments. The Celligen was placed in its stand and autoclaved (in a large autoclave) for 30 min.

Step 9: The Celligen reactor was removed from the autoclave whereupon the loosened clamps were immediately tightened. The bioreactor was allowed to cool and the

DO probe was immediately attached to the console to allow for charging before it was calibrated. The thermister well was filled with glycerol at this point.

Step 10: The pH electrode was checked by removing the plugs in the fill ports and checking the pH reading for the PBS within the vessel. If the reading was off slightly it was readjusted to read the appropriate value. The PBS was then removed from the vessel aseptically and 1-1.1 L of fresh medium was added.

Step 11: The temperature of the medium was allowed to equilibrate, and the agitation turned on. The DO probe was then calibrated by sparging the medium with nitrogen gas (more soluble than O₂ in water) for 30 min whereupon the console was given a zero value of dissolved oxygen. Subsequently, the medium was sparged with air for 30 min which gave a 100% value for dissolved oxygen. Once the DO probe was calibrated, the medium was again allowed to equilibrate with the optimal gas (air, N₂, CO₂ and O₂) proportions.

Step 12: Cytodex-1 microcarriers were utilized (purchased from Pharmacia Biotech Co.). These microcarriers are based on a cross-linked dextran matrix which is substituted with positively charged N, N-diethylaminoethyl groups. These charged groups are distributed throughout the microcarrier matrix. The bead itself has an area of 4400 cm²/g dry weight, and a diameter of 190 µm. The microcarriers were hydrated in PBS for 24 hr (they have a swelling factor of

20 ml/g dry weight) and rinsed with fresh PBS. The beads were autoclaved for 15 min and resuspended in sterile medium.

Step 13: 15 large petri dishes of MLC or HKC were harvested aseptically and placed in 150 ml of medium. The cells were added to the microcarriers and allowed to equilibrate (attach to the carriers) for 2-3 hrs before addition to the Celligen reactor.

Step 14: The agitation was turned off and the cells, along with the carriers were added aseptically to the Celligen via the addition port. A special sterile addition vessel equipped with silicon tubing and a glass adapter (male) containing the cells was attached to the female adapter of the addition tubing (adapters were swabbed with ethanol and flamed before during and after attachment). The clamps were then removed and the cells were allowed to siphon into the Celligen. Fresh medium (30 ml) was subsequently added to flush down any remaining cells. Once addition was completed, the addition vessel was detached and the addition port tubing was clamped shut. The agitation was kept off overnight and increased to 60 rpm the subsequent day.

2.1.5 Biotransformation

Biotransformation Conditions: The cells were allowed to proliferate for 7-10 days at 60-80 rpm, pH 7.4, DO of 50% and a temperature of 37 °C in the Celligen. At this point enough cells were present for biotransformation. The substrate was

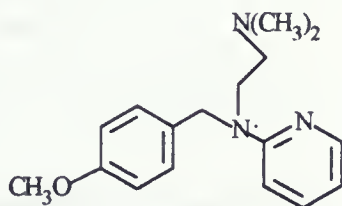
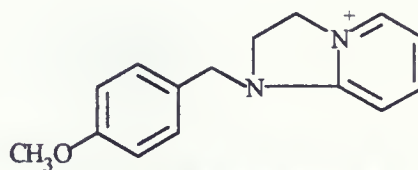
added in dialysis tubing as previously mentioned and biotransformation was halted after 4 days. 100 mg/L of pyrilamine maleate, 160 mg/L of spironolactone and 300 mg/L of chloramphenicol were used for biotransformation, determined from the specific toxicity threshold for each pharmaceutical.

2.1.6 Product Recovery

Medium Manipulation: The cells in the Celligen were allowed to settle and the medium was harvested and placed on a continuous extractor for 3-4 days with dichloromethane and 0.5 ml antifoam. The extract was collected, dried with MgSO_4 and evaporated to dryness.

Product Isolation: The crude extract was purified using a chromatotron. A 2 mm thick silica disk (Silica gel 60 PF₂₅₄, Merck) was prepared capable of loading up to 300 mg of crude product. The sample was dissolved in the solvent system of choice (determined by TLC) and added to the disk while spinning. Band separation was visible by UV light and desired bands were collected in 125 ml Erlenmeyer flasks as pure fractions and evaporated to dryness.

Pyrilamine Maleate extract: The crude extract was purified using 87% chloroform: 13% 9:1 MeOH: NH_4OH gradient which removed any starting material [1]. The gradient was increased to 50% MeOH: 50% NH_4OH which eluted the highly polar metabolite [2].

**1** Pyrilamine Maleate**2** Pyrilamine Metabolite

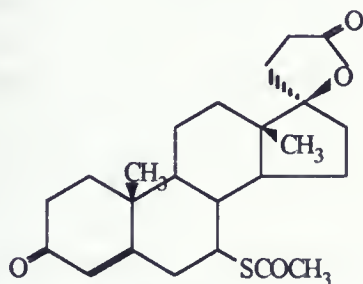
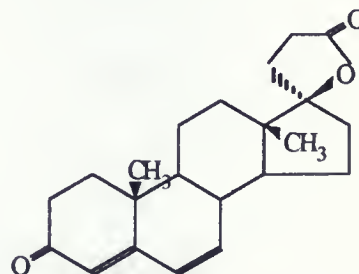
Pyrilamine Maleate [1] $^1\text{H-NMR}$: (CDCl_3 , 300MHz); δ 2.25 (6H, s, $(\text{CH}_3)_2$), 2.50 (2H, t, CH_2), 3.62 (2H, t, CH_2), 3.78 (3H, s, OCH_3), 4.69 (2H, s, CH_2), 6.48 (1H, m, aromatic), 6.82 (1H, d, aromatic), 7.10 (1H, d, aromatic), 8.10 (1H, m, aromatic)

MS [EI +] m/z (RI%); 285 [M^+] (5%), 214 [$\text{M}-(\text{CH}_2)_2\text{N}(\text{CH}_3)_2$] $^+$ (11.9%), 121 (100%), 58 (58.9%)

Pyrilamine Metabolite [2] $^1\text{H-NMR}$: (CDCl_3 , 300MHz); δ 3.81 (3H, s), 4.02 (2H, t), 4.3 (2H, t), 4.61 (2H, s), 6.91, 7.28, 7.85, 8.81, (aromatic)

MS [FAB+] m/z (RI%); 241 [M^+] (34.2%), 207 (30.6%), 115 (100%)

Spironolactone extract: The crude extract was purified using 80:20 hexane:ethyl acetate gradient which eluted the major metabolite, canrenone [4] in 70% yield.

**3** Spironolactone**4** Canrenone

Spironolactone [3] $^1\text{H-NMR}$: (CDCl_3 , 300MHz); δ 1.0 (3H, s, CH_3 -18), 1.2 (3H, s, CH_3 -19), 2.3 (3H, s, S-COCH_3), 2.8 (2H, dq, C-6H), 3.9 (1H, q, C-7H), 5.7 (1H, s, C-4H)

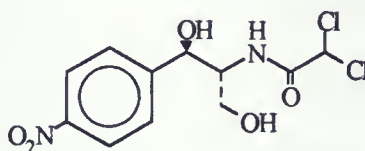
^{13}C -NMR: (CDCl_3 , 75 MHz); (198, 194, 176, 165, CO), (14 -49, 18 peaks, steroid structure), (95, 126, C=C)

MS $[\text{EI}^+]$ m/z (RI%): 416 $[\text{MI}^+]$ 2%, 340 $[\text{SCOCH}_3]$, 32.3%

Canrenone [4] ^1H -NMR: (CDCl_3 , 300MHz); δ 1.0 (3H, s, CH_3 -18), 1.2 (3H, s, CH_3 -19), 5.7 (1H, s, C-4H), 6.2 (2H, q, $\text{HC}=\text{CH}$)

MS $[\text{EI}^+]$ m/z (RI%): 340 $[\text{MI}^+]$ 41.4%

Chloramphenicol [5] extract: The crude extract was purified using 9:1 ethyl acetate: methanol gradient respectively which eluted the starting material fraction.



5 Chloramphenicol

Chloramphenicol [5] ^1H -NMR: (CD_3OD , 300MHz); δ 3.32 (1H, s, NH), 3.63 (1H, q OH), 3.83 (1H, m, CH), 4.15 (1H, m, CH), 4.89 (3H, s, CH_2), 5.12 (1H, d, OH), 6.25 (1H, s, CHCl_2), 7.67 (2H, d, aromatic), 8.20 (2H, d, aromatic)

MS $[\text{EI}^+]$ m/z (RI%): 323 $[\text{MI}^+]$ 99%, 305 $[\text{OH}]$ 39%, 275 $[\text{OH}]$ 40.3%

2.1.7 Toxicity Assays

Pharmaceutical Threshold: The toxicity threshold of the pharmaceutical substrates pyrilamine, and spironolactone were determined by cultivating cells in their normal growth medium in 14 ml petri dishes. The cells were grown to confluence and fresh medium containing the pharmaceutical in a known

concentration was added to each plate. Concentrations of 0.85 mM, 0.5 mM, 0.36 mM, 0.18 mM and 0.11 mM along with a control were tested for both drugs. The concentrations tested were chosen according to previously estimated thresholds such that concentrations above and below this value were chosen. The cells were incubated for 48 hr, and subsequently observed under a light microscope to determine the viability of the cells. In addition, pertinent plates were harvested and reseeded to determine the extent of viability.

Optimal reagent concentrations for encapsulation:

MOPS buffer: Twelve petri dishes containing confluent cells were exposed to 0, 0.105 mM, 0.175 mM, 0.28 mM, 0.30 mM, and 0.35 mM MOPS buffer and observed after 48 hr for viability. Three different solutions of MOPS were tested; MOPS in water, MOPS in DMEM, and MOPS in PBS.

PAA: The optimal concentration of PAA was determined through trial and error via capsule formation. The amount of PAA utilized must be in a certain molar ratio with the amount of MOPS buffer utilized. In addition, the concentration of PAA cannot be too small since mechanically unstable capsules are obtained. By manipulating these variables, and observing the quality of capsules obtained, the concentration of PAA utilized was arrived at and found to be 0.076 M.

Span 85: Through trial and error, the minimum amount of Span 85 required to form an appropriate emulsion without causing aggregation of capsules was determined to be 300 μL .

Acid Chloride: Once the quantities of MOPS and PAA were determined, the amount of acid chloride was adjusted according to a set mole ratio and found to be 17 μL .

2.1.8 Preparation of Starting Material

Pyrilamine free base: Pylamine maleate (100 mg) was placed in saturated NaHCO_3 and extracted 3X with dichloromethane. The organic layer was dried with MgSO_4 and the residue evaporated to dryness.

2.2 *Rhodococcus rhodochrous* Project

2.2.1 Growth Conditions

Rhodococcus rhodochrous ATCC 17895 was grown in a liquid medium consisting of 15 g/L glucose, 5 g/L bactopectone, 1 g/L yeast extract, 0.5 g/L MgSO_4 , 1.2 g/L K_2HPO_4 , 0.7 g/L KH_2PO_4 supplemented with 1 g/L caprolactam and 0.01% (w/v) FeSO_4 . The buffer component was autoclaved separately and added to the sterile medium afterward to avoid precipitation of salts. Caprolactam and FeSO_4 were added to the prepared medium through a sterile filter. These

components are vital for inducing the nitrile hydratase enzymes in *Rhodococcus rhodochromus*. Once the medium was sterilized, mixed and supplements added, inoculation from agar plates (composed of 8 g/L Nutrient Broth and 15 g/L Bactoagar) containing cultured *Rhodococcus* sp. using a sterile loop was performed. The 500 ml flasks were then incubated at 27 °C on a rotary shaker set at 180 rpm for 48 hr.

Cells were recovered during the stationary phase of growth by harvesting the medium into 250 ml centrifuge bottles and centrifuging for 20 min at 4 °C, 10,000 rpm. The supernatant was subsequently decanted and the pellets washed in 0.5 M tris buffer, pH 7.2 or 7.8 and centrifuged again. The buffer was decanted and the wet pellets weighed. The pellet was resuspended in the appropriate amount of Tris to give a concentration of 100 mg wet weight/ml. Cells were either frozen in sterile 50 ml centrifuge tubes or used immediately for biotransformation.

2.2.2 Free Cell Biotransformation

Harvested cells (frozen or fresh) in a concentration of 100 mg wet weight/ml 0.5 M TRIS, pH 7.2 were placed in a 250 ml Erlenmeyer flask to which 4 mg/ml of neat substrate was added after the flask was equilibrated at the appropriate temperature.

Heptyl nitrile: Biotransformation was performed at 27 °C, 180 rpm using fresh and/or frozen cell preparations and monitored until reaction completion (3 hr).

1 ml samples were taken every 10 min and analyzed by gas chromatography (GC).

2-(4-chlorophenyl)-3-methylbutyronitrile (CPIN): Biotransformation was performed at 32 °C, 180 rpm using fresh cell preparations and monitored for the duration of the reaction (5 days). 1ml samples were taken every 3 hr for the first 24 hr and once every subsequent day. Samples were analyzed by GC.

Controls: Control experiments for heptyl nitrile and CPIN compounds in aqueous buffer were performed. The desired compound (20 µl), was placed in 20 ml Tris buffer in a 50 ml Erlenmeyer flask at 32°C, 180 rpm for CPIN, CPIN amide, and CPIN acid and 27 °C, 180 rpm for heptyl nitrile, octyl amide, and octanoic acid. Aliquots (0.5 ml), were extracted into ethyl acetate after acidification and examined by GC. Samples were taken every day for up to 7 days.

2.2.3 Two-phase Biotransformation

Rhodococcus rhodochrous cells were harvested as previously stated (100 mg wet weight/ml of 0.5 M Tris, pH 7.2) and placed in the presence of a certain volume ratio of octane/buffer. The cell suspension was equilibrated in a shaker at 180rpm and 4mg/ml neat substrate was subsequently added.

Heptyl nitrile: Biotransformation was performed with a 50:50 (v/v) ratio of aqueous to organic layer. Fresh and/or frozen cell preparations were used and

the reaction performed at 27 °C, 180 rpm. Aliquots (1 ml) from the aqueous and organic phases were taken every 10 min and analyzed by GC over a period of 3 hr.

CPIN: Biotransformation was performed with a 1:5 (v/v) ratio of organic to aqueous layer, respectively. Fresh cell preparations were used and the reaction was performed at 32°C, 180 rpm. Aliquots (1 ml) from the aqueous and 0.5 ml aliquots from the organic layer were taken every 3 hr for the first 24 hr and once every subsequent day for 5 days. The samples were analyzed by GC.

2.2.4 Encapsulated Biotransformation

Encapsulation methodology is as previously mentioned in section 2.1.2. The concentration of each component was altered for bacterial encapsulation. 0.5M tris (tris(hydroxymethyl)aminomethane), pH 7.8 was utilized in lieu of MOPS buffer due to the low tolerance *Rhodococcus* sp. has for MOPS. The concentrations and quantities of the reagents are given in Table 2.

Table 2: Quantities used for encapsulation of *Rhodococcus* sp.

Reagent	Volume	Concentration
Cells	1.5ml	100mg/ml
Tris	1.5ml	0.5M, pH 7.8
PAA	---	0.133M
Octane	15ml	----
acid chl.	0.04ml	----
Octane (dry)	15ml	----
Span 85	0.35ml	----

The procedure was performed on ice, and cured capsules were rinsed with octane and resuspended in octane/toluene for biotransformation.

Heptyl nitrile: Biotransformation performed at 27 °C, 80 rpm, for 48 hr in the presence of 4 mg/ml substrate. Samples were analyzed by GC.

CPIN: Biotransformation performed at 32 °C, 80 rpm, for 7 days in the presence of 4 mg/ml CPIN. Samples were analyzed by GC.

2.2.5 Viability Studies

Sterile loop inoculation of free cell and two-phase biotransformations onto nutrient broth agar plates was performed every day during conversion. The presence of proliferating cells was indicative of cell viability. For encapsulated systems, capsules were disrupted via sonication and plated along with capsular debris immediately after capsule formation. The plates were observed for possible proliferation and plated once again on fresh nutrient broth agar plates for confirmation of observations in the absence of capsular debris.

2.2.6 GC Analysis

Aliquot (1 ml) samples were placed in 2 ml centrifuge tubes, whereupon the reaction was halted by lowering the pH to 2 with the addition of 150 µl of 5% aqueous HCl. The starting material and product(s) were extracted into 0.5 ml ethyl acetate which contained 1 mg/ml of the internal standard. Samples were

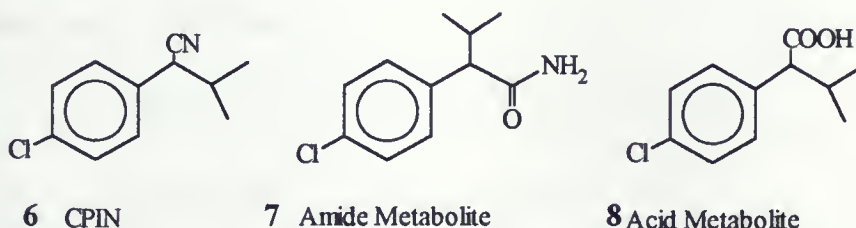
vortexed for 30 sec and centrifuged at 1500 rpm for 1 min. Injections (1 μ l) of the extract were analyzed by GC. A Hewlett Packard-5890 Capillary Gas Chromatograph equipped with a Flame Ionization Detector (FID) was utilized. This dual column, dual inlet instrument contains a 15m x 0.53mm I.D. megabore column with the stationary phase being composed of 5% phenyl-95% dimethyl polysiloxane (DB5) with a film thickness of 1.5 μ m. High purity helium gas was used as the carrier gas and the make-up gas for the FID. High purity hydrogen and air were used as the fuel and oxidant respectively for the FID. A Hewlett Packard Chromatography Station program was utilized for data acquisition, processing and output.

Heptyl nitrile analysis: The internal standard for this analysis was decane (b.p. 174 °C). Conditions used: Initial temperature (IT): 75 °C, Rate: 10 °C/min, Final Temperature (FT): 150 °C, Equilibration Time (ET): 0.5 min, Injector Temperature (INT): 200 °C, Detector Temperature (DT): 250 °C, Purge Time (PT): 0.1 min, injection: 1 μ l. Retention Time (RT) decane, 2.99 min; heptyl nitrile, 4.03 min; octanoic acid, 5.23 min; amide, 7.79 min

CPIN analysis: The internal standard for this analysis was trichlorotoluene (b.p. 248°C). Conditions used: IT: 110 °C, Rate: 15 °C/min, FT: 220 °C, Final Time: 15 min, ET: 0.5 min, INT: 250 °C, DT: 250 °C, PT: 0.1 min, injection: 1 μ l. RT trichlorotoluene, 4.23 min; CPIN, 5.57 min; CPIN acid, 6.34 min; CPIN amide, 7.55 min

2.2.7 Product Recovery and Isolation

The medium from a large scale free-cell biotransformation of CPIN [6] was collected, acidified with 5% HCl, and centrifuged to remove the cells. The medium was put on a continuous extractor with dichloromethane for 3 days whereupon the extract was dried with MgSO_4 and evaporated to dryness. The crude extract was purified on a silica gel column using 70:230 mesh Silica from Aldrich. Approximately 100 ml silica slurry was prepared in 6:1 hexane:ethyl acetate. Pure amide [7] and acid [8] were recovered in 30% yield.



CPIN [6] $^1\text{H-NMR}$: (CDCl_3 , 300MHz); δ 1.07 (6H, dd, $(\text{CH}_3)_2$), 2.10 (1H, m, CH), 3.67 (1H, d, CH), 7.27 (2H, d, aromatic), 7.38 (2H, d, aromatic)

$^{13}\text{C-NMR}$: (CDCl_3 , 75MHz); 19.11, 21.11, 34.18 (CH_3), 44.92 (CH_3), (119.82, 129.60, 133.82, aromatic), 134.39 (CN)

MS [EI^+] m/z (RI%); 193 [M^+] 10.2%, 151 [$(\text{CH}_3)_2$] 100%, 116 [Cl] 9.7%, 89 [CN] 12.3%

Amide Metabolite [7] $^1\text{H-NMR}$: (CDCl_3 , 300MHz); δ 0.70 (3H, d, CH_3), 1.09 (3H, d, CH_3), 2.35 (1H, m, CH), 2.90 (1H, d, CH), 5.51 and 5.70, broad (1H singlets, NH_2) 7.3 (4H, s, aromatic)

$^{13}\text{C-NMR}$: (CDCl_3 , 75MHz); 20.59, 21.89, 31.84 (CH_3), 60.87 (CH_3), (129.98, 133.56, 137.85, aromatic), 176.06 (C=O)

MS [EI⁺] m/z (RI%): 211 [MI⁺] 25.6%, 169 [C(CH₃)₂] 100%, 125 [CONH₂] 97.2%

IR: 1680cm⁻¹ (C=O, sharp peak), (2873cm⁻¹, 2933cm⁻¹, 2933cm⁻¹, CH₃) 3200cm⁻¹, 3350cm⁻¹ (NH₂)

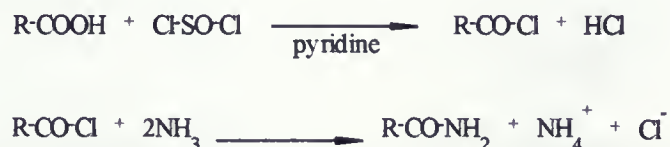
Acid Metabolite [8]¹H-NMR: (CDCl₃, 300MHz): δ0.70 (3H, d, CH₃), 1.10 (3H, d, CH₃), 2.35 (1H, m, CH), 3.2 (1H, d, CH), 7.3 (4H, s, aromatic)

¹³C-NMR: (CDCl₃, 75MHz); 20.57, 21.76, 31.81 (CH₃), 60.98 (CH₃), (129.10, 133.77, 137.54, aromatic), 179.61 (C=O)

MS [EI⁺] m/z (RI%): 212 [MI⁺] 26.3%, 170 [C(CH₃)₂] 100%, 125 [COOH] 40.4%

IR: 1680cm⁻¹ (C=O, sharp peak), (2873cm⁻¹, 2933cm⁻¹, 2933cm⁻¹, CH₃), 3000cm⁻¹ (COH, broad peak)

2.2.8 Preparation of Materials

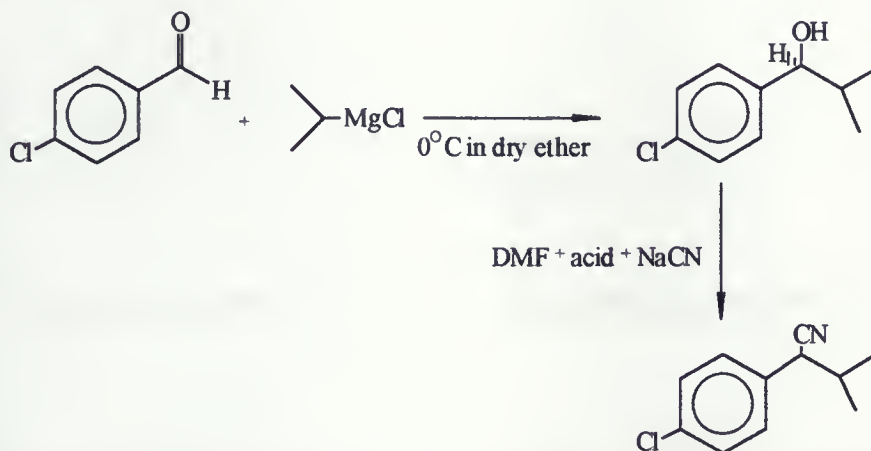


Scheme 2: Synthesis of octyl amide via an acid chloride intermediate

Synthesis of octyl amide (scheme 2): A mixture of 1.44 g octanoic acid, 1.44 g thionyl chloride, and one drop of pyridine were added to 50 ml dry benzene in a round bottom flask. The flask was attached to a condenser containing a drying tube and refluxed for 2 hr. The solution was then evaporated to dryness and 20 ml conc. NH₃ was added and stirred for 1 hr. The reaction mixture was extracted into ethyl acetate and washed with NaHCO₃ and water. The extract was dried with MgSO₄ and evaporated to dryness. The crude product was

recrystallized with ethyl acetate and washed with ethyl ether. A yield of 95% was obtained.

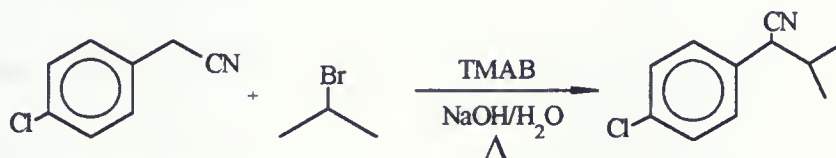
Octyl amide $^1\text{H-NMR}$: (CDCl_3 , 300MHz); δ 0.90 (3H, t, CH_3), 1.33 (8H, d), 1.66 (2H, quintet, CH_2CO), 2.25 (2H, sextet, CH_2CO), 5.41 (2H, broad singlet, NH_2)



Scheme 3: Attempted synthesis of CPIN via Grignard Reaction

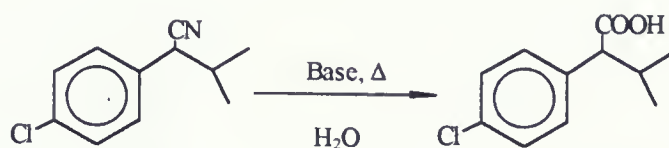
Synthesis of CPIN via Grignard Reaction (Scheme 3): A solution of 4-chlorobenzaldehyde (5 g, 0.0356 moles) in 50 ml dry ether was placed in a round bottom flask and cooled to 0°C . Isopropylmagnesium chloride (4.5 ml, 0.03556 moles) was added anhydrously through a syringe over 20 min. The reaction was stirred overnight at room temperature. HCl (5%) was then added to the reaction mixture and an extraction with ether was performed. The ether layer was dried with MgSO_4 and evaporated to dryness. A crude NMR revealed low yield of product and procedure was modified to include benzaldehyde in lieu of chlorobenzaldehyde in an attempt to minimize side reactions. In this

case, 5 ml (0.0471 moles) of benzaldehyde was used in 50 ml of dry ether. The grignard reagent was added in excess (10 ml, 0.0942 moles) and the reaction was refluxed overnight. Again, crude NMR showed minimal product, such that purification and progression of material to the next step was abandoned.



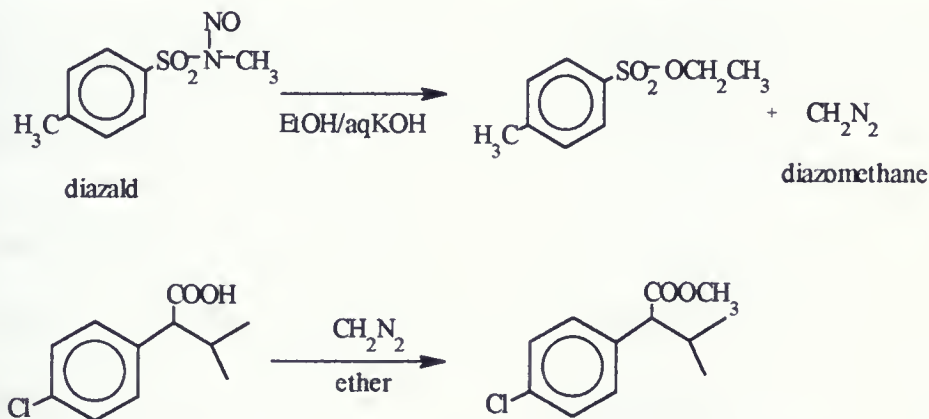
Scheme 4: Synthesis of CPIN using industrial approach (32)

Synthesis of CPIN using industrial approach (Scheme 4) (32): In a round bottom flask, 16 g 50% (w/w) NaOH:H₂O and 0.3435 g tetramethylammonium bromide (TMAB), a phase transfer catalyst, were mixed thoroughly. Once completely dissolved, 15.1 g 4-chlorobenzyl cyanide was added and stirred. 2-bromopropane (16 g) was added over an hour while maintaining the temperature at 45 °C. After addition, the reaction was refluxed overnight at 60 °C (32). Upon completion of reaction, 20 ml of ether was added to the flask and the aqueous layer was removed in a separatory funnel. The ether layer was washed 3X with water, dried with MgSO₄ and evaporated to dryness. (For spectral details, see page 63)



Scheme 5: Synthesis of CPIN acid by chemical hydrolysis

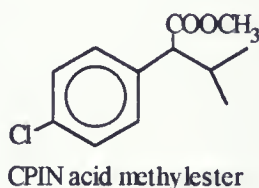
Synthesis of CPIN acid (Scheme 5): CPIN (150 mg) in 40 ml of 50:50 (v/v) 25% KOH: ethanol was placed in a round bottom flask and refluxed for five days. The mixture was cooled, acidified to pH 1. The ethanol was removed by roto-evaporation and the residue was extracted into chloroform. The extract was dried with MgSO_4 and evaporated to dryness. (For spectral details see page 63).



Scheme 6: Preparation of CPIN acid methyl ester

Derivatization of CPIN acid to methyl ester (scheme 6): The two reactions depicted in scheme 6 were performed simultaneously in separate flasks. As diazomethane was generated in one flask, it was distilled into a receiving flask where reaction with the CPIN acid occurred. The distillation flask was charged with a solution

of 5 g KOH in 8 ml of water and 25 ml 95% ethanol. The flask was heated to 65 °C with a steam bath and a 0.1 mole solution of *p*-toluenesulfonylmethylnitrosoamide (diazald) was added dropwise to 130 ml ether over 20 min. The receiving flask contained 50 mg CPIN acid in 30 ml of 50:50 methanol:ether. Excess diazomethane was neutralized with acetic acid.



CPIN acid methyl ester: $^1\text{H-NMR}$: (CDCl_3 , 300MHz); δ 0.70 (3H, d, CH_3), 1.0 (3H, d, CH_3), 2.25 (1H, m, CH), 3.15 (1H, d, CH), 3.7 (3H, s, OCH_3), 7.3 (4H, s, aromatic)

2.2.9 Chiral analysis

Chiral analysis was performed on a Chiraldex G-BP column with the dimensions of 30 m x 250 μm and 0.13 μm film thickness. Neat racemic standards and experimental samples were dissolved in dry dichloromethane in a concentration of 5 mg/ml, where 0.1 μl of sample was injected. Acid functionalities must be derivatized for analysis, hence the methyl ester of CPIN acid was prepared using diazomethane (see scheme 6). Enantiomeric excess was determined using the formula:

$$\frac{E_1 - E_2}{E_1 + E_2} \times 100\%$$

where E_1 and E_2 are the peak areas of enantiomers 1 and 2 respectively.

CPIN analysis: flow rate: 1.3 ml/min, split ratio: 100:1, isochratic temperature: 140 °C, retention times: 16.46 min, 16.956 min

CPIN amide analysis: flow rate: 1.3 ml/min, split ratio: 100:1, isochratic temperature: 220 °C, retention times: 12.057 min, 12.494 min

CPIN acid methylester analysis: flow rate: 0.7 ml/min, split ratio: 100:1, isochratic temperature: 130 °C, retention times: 8.980 min, 9.177 min

Chapter 3: Results and Discussion

3.1 Mammalian Cell Culture Project

Encapsulation via interfacial polymerization as described in section 2.1.2 was initially performed with human kidney cells (HKC). Previous work encapsulating HKC proved unsuccessful, and it was postulated that the cells were perishing because they had no place to anchor themselves. This anchorage-dependent cell line was allowed to adhere to microcarriers and an attempt was made to encapsulate these cell-containing carriers. The viability of the cells was not improved by using the microcarriers.

A mouse liver cell line (MLC), which is semi-anchorage dependent, was investigated as an alternative route to successful mammalian cell encapsulation.

3.1.1 Encapsulation of Mammalian Cells

Several components of the encapsulation procedure were modified and optimized specifically for the MLC. A toxicity assay for MOPS buffer was initially performed in order to deduce the maximum concentration the MLC could withstand. Three different media were also tested for effect on the cells.

Referring to Table 3, the observations and results for this experiment are shown.

Table 3: Results from MOPS Toxicity Assay

[MOPS]	IN DMEM	IN PBS	IN H ₂ O
CONTROL	+++++ very confluent, many adherent cells as well as in suspension	++++ sparse adherent cells, smaller quantity of cells in suspension	++ sparse cells, few adherent
0.105M	++++ many adherent cells, good amount in suspension	++ few adherent cells, few in suspension	++ sparse cells, few adherent
0.175M	++++ many viable cells, good amount in suspension	++ few adherent, large aggregates in suspension	+ large aggregates, sparse cells, non adherent
0.280M	++++ many viable cells, good amount in suspension	++ few adhered, small aggregates in suspension	++ no adherent cells, single cell suspensions, cells looked smaller
0.30M	+++ small dense aggregates in suspension, some adherent cells	_____	_____
0.35M	++ small single cell suspension, few adherent cells	_____	_____

**** +: Increasing + signs reflects amount of viable cells present upon visual examination of cell samples under a light microscope**

MLC grow in suspension as well as attached to a surface, healthy and/or viable cells were judged based on the amount which adhered as well as the quantity of cells in suspension. The quality of the aggregates which MLC produce in suspension also dictates viability. Unusually large aggregates may indicate cell

death while extremely small aggregates may indicate poor viability as well. Intermediate aggregates in conjunction with the presence of adherent cells are characteristic of viable cell growth. From Table 3, it is evident that MOPS buffer prepared in water alone will not cultivate healthy cells. MOPS in PBS showed cell proliferation, but not as vigorous as those cells present in MOPS/DMEM medium. Hence, this medium was chosen as optimal. The toxicity threshold of MOPS in DMEM appeared to be either 0.28 M, 0.30 M or 0.35 M. These plates were harvested and reseeded to observe proliferation ability after exposure to MOPS. It was determined that 0.28 M MOPS contained the most robust cells due to its extensive proliferation after reseeding.

According to Khan *et al.*(7), the original concentrations of reagents for encapsulation of yeast cells were as listed in Table 4; the tailored concentrations and quantities which were used for encapsulation of MLC are given in Table 5.

Table 4: Quantities of Reagents for Encapsulation of Yeast Cells (7)

Reagent	Volume	Conc.
Cells	0.5ml	*37.5mg/ml
MOPS	1.5ml	0.75M, pH7.8
PAA	-----	0.2M
Decane	15ml	-----
Acid Chl.	45 μ l	-----
An. Decane	15ml	-----
Span 85	420 μ l	1.4% (v/v)

*dry weight, An. = anhydrous

Table 5: Quantities of Reagents for Encapsulation of Mammalian Cells

Reagent	Volume	Conc.
Cells	-----	10^8 cell/ml
MOPS	2.0ml	0.28M
PAA	-----	0.076M
Hexadecane	20ml	-----
Acid Chl.	17 μ l	-----
An.Hexadec.	15ml	-----
Span 85	300 μ l	1.0% (v/v)

Upon comparison, lower concentrations and volumes of reagents were used for mammalian cell encapsulation. Due to the toxicity threshold of MOPS for MLC, lower amounts of PAA and acid chloride were adopted to satisfy the mole ratio of 17:83 MOPS:PAA, respectively. PAA and the acid chloride are used as a 1:1 mole ratio for yeast cell encapsulation, this was reduced to 0.8 mole acid chloride to 1 mole PAA for mammalian cells. In doing so, the amount of excess hydrogen chloride produced was minimized. In addition, the quantity of Span 85 was lessened such that a suitable emulsion was obtained, without an excess amount. The amount of MLC used was changed from the initial 10^6 cells/ml assay to 10^8 cells/ml to produce capsules which contained a larger number of cells in an attempt to increase overall viability.

Referring to Figure 21 , the polyamide capsules which were produced using MLC or human kidney cells are approximately 120 μ m in size.

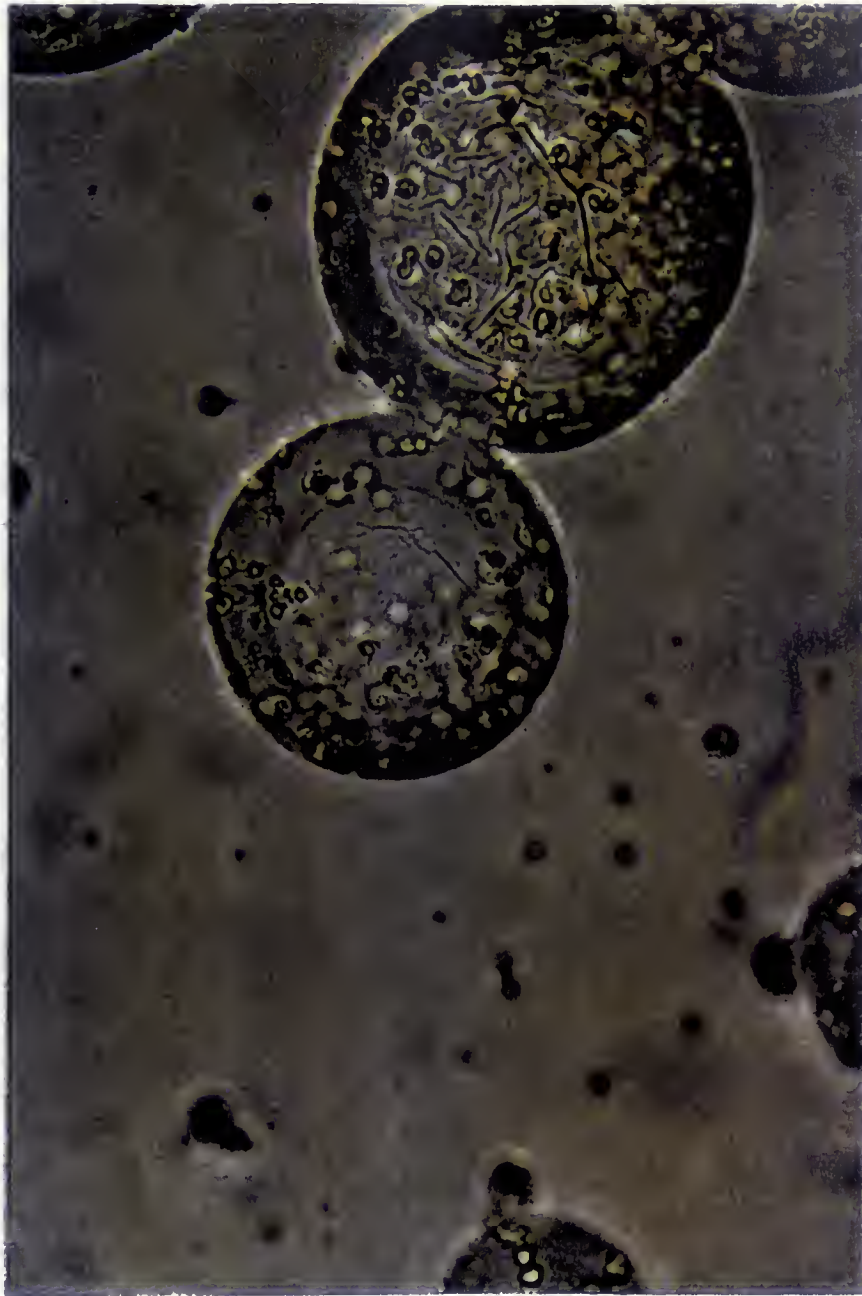


Figure 21: Microencapsulated human cells as seen under a light microscope (10X). Approximate size of capsules: 120μm
Photo by G. Stroffolino

3.1.2 Viability Determination

Once conditions were optimized, and mechanically stable capsules were obtained, the viability of the MLC within the capsules had to be determined. One approach was to disrupt the capsules themselves. Several procedures were developed to allow one to harvest, wash, and disrupt the capsules without damaging the cells in the process. Harvesting was performed aseptically so as not to infect the delicate cells and to remove the capsules from the hexadecane solvent. Afterward, the capsules were washed to remove trace amounts of solvent which would potentially come into contact with the cells upon capsule disruption. A second method was to perform a biotransformation and analyze the reaction for product formation. The third, and most successful method involved viability staining using a fluorescent dye.

Capsule Disruption

Method development for harvesting, washing and disrupting the microcapsules was required before viability of the cells could be determined. The first method involved gravity filtration of the solvent using Kimwipes as a sieve which would collect the capsules. The capsules were washed with sterile DMEM medium and sonicated for 2.5 min. The process of sonication disrupts the capsular membrane without harming the cells. Verification of this fact was obtained when fresh MLC were harvested, resuspended in DMEM and

sonicated for 2.5-3.0 min. These cells were reseeded and found to proliferate normally after sonication. Once the capsules were broken, an aliquot of the sonicated sample was viewed under a light microscope using the dye exclusion stain, trypan blue. This stain relies on the ability of living cells to exclude the dye from crossing the membrane. Dead cells, with their cell membranes being compromised, are permeable and will take up the stain.

Gravity filtration was not an ideal method for capsule isolation since significant amounts of hexadecane remained. In addition, washing with DMEM alone did not remove the excess solvent. Hence, once capsules were disrupted, the sample contained a small emulsion of hexadecane along with the capsular debris. When stained and viewed under a light microscope, it was difficult to determine viable cells from the small fragments of capsular debris. In addition, the debris itself was prone to staining by the dye. As a result, the viability of the cells remained inconclusive.

The harvesting of microcapsules was enhanced by the use of a cellular sieve and light suction filtration in place of the Kimwipe and gravity filtration. This removed ample amounts of hexadecane. The washing procedure was modified by the addition of a surfactant to remove any solvent which remained after filtration. Several solutions of surfactants in PBS were tested, among which were 1% (v/v) tween 20, 1% (v/v) span 85, and 0.01% (v/v) sodium dodecyl sulphate (SDS). 0.01% SDS succeeded in removing solvent without

aggregating the capsules and causing an emulsion. Hence, the washing procedure included rinsing 1X with 0.01% SDS, and 3X with DMEM.

This method allowed larger fragments of capsular debris to be filtered out, consequently when samples were viewed under the light microscope, a higher degree of clarity between cells and debris was obtained. However, small particulates which remained, made it difficult to see viable versus nonviable cells with trypan blue staining. As a result, another approach to viability determination was taken.

Biotransformation

Viability could also be determined by enzymatic activity of a specific reaction. By monitoring the formation of product during biotransformation, the whole process of capsule disruption without harming the cells would be evaded. Hence, bioconversion of pyrilamine maleate (see experimental, structure 1), an ethylenediamine-type antihistamine was investigated.

First, a toxicity assay for the drug was performed, the results of which are presented in Table 6. The toxic threshold for 100% survival was determined to be 0.25 mM which translates to 8.53×10^{-8} mg/cell. DMEM was again, a more suitable medium to use for biotransformation.

Table 6: Toxicity Assay for Pyriline Maleate

[Pyriline Maleate]	IN DMEM	IN PBS
Control	+++++ very confluent cells	++++ confluent cells
0.11mM	+++++ similar to control	++ very sparse growth
0.25mM	++++ good proliferation	++ sparse growth
0.36mM	+++ large aggregates, few adherent cells	++ sparse growth, some adherent cells
0.51mM	++ very few adherent cells	+ few adherent cells
0.85mM	+ majority of cells are dead	0 no viable cells

Biotransformation in a free cell system yielded 90% conversion to the pyriline metabolite (see experimental, structure 2). The encapsulated biotransformation was performed in saturated hexadecane at 37°C, 100rpm for 72hr. Extraction of the hexadecane solvent with water and re-extraction of the aqueous layer with dichloromethane isolated any potential products. Analysis of the internal aqueous capsule environment and the hexadecane solvent by TLC revealed the presence of starting material alone ($R_f = 0.78$, 8.7:1.3 CHCl_3 : $\text{MeOH:NH}_4\text{OH}$ (9:1)).

Research as to why there was no biotransformation of pyriline maleate in the encapsulated system lead to testing of several variables such as permeability, oxygen availability, and buffering capacity. To test the permeability of the substrate through the capsular membrane, empty capsules

were prepared which were subsequently incubated overnight with pyrillamine maleate in hexadecane. Analysis of internal/external environments of the capsules by thin layer chromatography (TLC) revealed the presence of substrate within the previously washed and sonicated capsules, suggesting no barrier to permeation.

Postulations that problems with oxygen solubility in the MOPS buffer was hindering oxygen delivery to the cells, rendering them dead was investigated. The solubility was tested by sparging 0.28M MOPS, pH 7.8 with air. A DO probe was used to measure the relative amount of dissolved oxygen before and after sparging. Levels of dissolved oxygen between 50-75% were detected over 2 hr. It was concluded that there was adequate solubility of oxygen in MOPS.

It was then hypothesized that the buffering capacity of a 0.28 M MOPS, pH 7.8 solution may be compromised during encapsulation by the production of HCl. The pH of the buffer is expected to lower up to 1 pH unit after encapsulation is complete because of acid production (7), however if the pH is lowered below 7.0, the cells will be in a non-physiological environment and thus perish. Again, empty capsules were prepared, washed, and disrupted by sonication. The debris was centrifuged and the pH of the internal MOPS was measured. It was found to be at a pH of 7, which is also sufficient for the cells. The logical conclusion to this is that the cells are not surviving long enough for

biotransformation to occur. What was still not known, was at which point were the MLC becoming damaged.

Viability Staining

To determine at which point during encapsulation, if any, the cells were losing their viability, a fluorescent dye was used instead of the trypan blue stain. Cells were stained at different stages before, and during encapsulation, the results of which are summarized in Table 7.

Table 7: Results of Viability Staining for MLC

Stage	%Viability
1	98%
2	74%
3	74%
4	NA

1= initial viability, 2= viability in the presence of DMEM/PAA,
3= after addition to hexadecane, 4= upon addition of acid chloride,
NA= not attainable

The mouse liver cells started the encapsulation process with a high viability. Upon addition of the cells to the DMEM/PAA/Gmax medium, the viability was reduced to 74% after 1 hr incubation. It may be possible that there is some static interaction between the amine polymer and the charged cell membrane which affects the cells unfavorably. The viability of the cells remained at 74% after addition to hexadecane, indicating that the cells have good tolerance for the solvent with short exposure. Once the acid chloride was

added however, viability of the cells was very low. Upon examination of the sample under the fluorescent microscope, cells were shown to form large aggregates which appeared to be attached to or intertwined with the capsular membrane, distorting the amount of cells present, and making an accurate viability count impossible. These cells, along with approximately 90% of the free cells on the slide were nonviable. The acid chloride may have had direct contact (through ionic interaction?) to the PAA- cell membrane complex (if formed) and disrupted the cells ionic balance, causing cells to lyse. It can thus be concluded that interfacial polymerization of MLC using a polyallyamide membrane which is created with PAA and acid chloride will not produce microcapsules with viable mammalian cells within.

3.1.3 Reverse Capsule Formation

Another approach for performing biotransformations of organic soluble substrates is to encapsulate the substrate itself as opposed to the cells. This provides increased stability and solubility to the substrate and allows the cells to exist in an aqueous environment.

Reverse capsules were prepared as mentioned in section 2.1.2, from a procedure developed by Khan *et al.* (7). Capsules produced by his group are shown in the electron micrograph in Figure 22. The procedure was modified

slightly from the original, which used larger amounts of acid chloride. It was found that upon stirring at high speeds with a motor driven overhead stirrer equipped with six 2 cm impeller blades, excessive foaming occurred. By reducing the amount of acid chloride slightly and lowering the speed from 2000 rpm to 1500 rpm, foaming was minimized and intact capsules could be obtained. Using MOPS buffer saturated with hexadecane also improved capsule formation. In addition to the procedure, the curing process was altered to include the addition of 0.01% SDS which lowered aggregation of the capsules. Formed capsules were stored in saturated MOPS buffer and observed for lifetime and manageability. It was found, after repeated experimentation, that the quality of the capsules produced was variable, with optimal results producing capsules which survived up to 4 days without aggregation. The mechanical stability was poor after this time period. The reverse-capsule process allows one to add the substrate along with the organic phase during capsule formation, but substrates which contain amine groups must be added afterward. Amine functionalities interfere with the polymerization process for membrane formation. Hence, these substrates, such as pyrillamine maleate must be added to fully formed capsules via diffusion. Addition of substrate in this



Figure 22: Reverse-phase capsules as seen under an electron microscope (10^6 amp). Approximate size of capsules: $30\mu\text{m}$
Photo by J.A. Khan

manner caused severe aggregation of the capsules rendering them unmanageable. A static charge may have been produced by the amine functionality attracting the capsules to one another. The idea for using these capsules in a bioreactor for bioconversion was considered impractical due to their instability.

3.1.4 Encapsulation Using Dialysis Tubing

The scenario of encapsulating the substrate as opposed to the cells still had possibilities. Since the reverse capsules were unstable, replacing them with dialysis tubing was attempted.

Dialysis tubing was filled with hexadecane and placed in $\text{Ca}^{2+}/\text{Mg}^{2+}$ free PBS for 24 hr. This certified that the capsule would not burst under osmotic pressure. Next, dialysis tubing containing hexadecane along with pyrilamine maleate was placed in PBS at 37 °C and 80 rpm overnight. The PBS layer was analyzed by TLC for the presence of pyrilamine maleate. TLC revealed that this substrate was capable of diffusing through the dialysis tubing into the aqueous environment. At this point, a small scale bioconversion of pyrilamine maleate was performed with dialysis tubing in a large petri dish containing confluent MLC. After 48 hr, the medium was partitioned with dichloromethane and analyzed by TLC, along with the hexadecane solvent within the tubing. Pylamine metabolite ($R_f=0.96$ in 8.7:1.3 CHCl_3 :MeOH/ NH_4OH (9:1)) was

detected in the medium, but not within the dialysis tubing. This was expected due to the high polarity of the product. Hence, this experiment gave indications that biotransformations performed in this manner were possible.

Before initiating a large scale biotransformation in the Celligen reactor (see experimental, pgs 45-51 for description), toxicity experiments as to solvent tolerance by MLC in dialysis tubing were performed. Large petri dishes containing confluent MLC were exposed to various solvents in dialysis tubing and observed for viability. Table 8 summarizes these results.

Table 8: Viability of MLC in the presence of solvents in dialysis tubing

Solvent	*Viability
hexadecane	18-20 days
toluene	12-13 days
octane	5-6 days
chloroform	0 days

* Viability is expressed as length of time, in days, required before 100% MLC death occurred

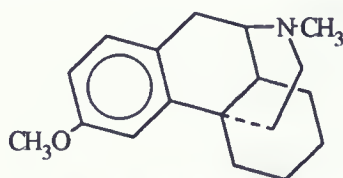
Hexadecane was the least toxic to MLC, allowing them to survive up to 18 days. Toluene was also examined due to its lower boiling point which makes recovery of products easier. Its toxicity was also good, allowing cells to survive for 13 days. Octane had higher toxicity, but still allowed the cells to survive for 5-6 days. The addition of chloroform to dialysis tubing caused the tubing itself to degrade, along with the petri dish containing the cells, hence, it proved to be a successful procedure for killing the MLC.

Dialysis tubing filled with hexadecane was placed in the Celligen reactor with distilled water. The agitation was turned on, and it was observed that the dialysis tubing did not interfere with the impeller. The tubing floated on the surface of the distilled water and moved in a circular motion around the impeller. With the initial leg-work completed, new substrates were tested for solubility in hexadecane, octane and toluene, as shown in Table 9.

Table 9: Solubility of pharmaceuticals in organic solvents and water

Compound (0.5mg/ml)	Hexadecane	Octane	Toluene	Water
Dextromethorphan	+++ slightly soluble	++ not very soluble	++++ soluble	++++ soluble
Spiro-lactone	++ not very soluble	+ insoluble	+++++ totally soluble	+ insoluble
Cholesterol-3-sulfate	++ not very soluble	++ not very soluble	+++ slightly soluble	+ insoluble
Chloramphenicol	++ not very soluble	+++ slightly soluble	+++ slightly soluble	++++ soluble

Dextromethorphan (9) (prepared as the HBr salt) is an antitussive and an antagonist of voltage dependent ion channels. Its structure is as follows:



9-Dextromethorphan

A toxicity assay for dextromethorphan revealed a toxic threshold of 0.18 mM (48.8 mg/L) or 4.1×10^{-8} mg/cell. This is fairly low since most drugs are tolerated at levels of 100 mg/L. A small scale biotransformation was performed, but due to the low amounts used, analysis of trace products could not be performed. Instead of scaling this biotransformation up, another compound with a higher toxicity threshold was chosen.

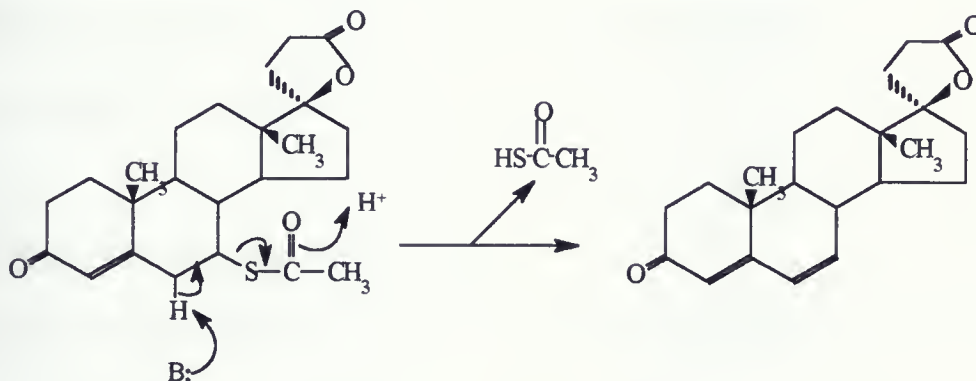
Chloramphenicol is an antibiotic originally isolated from *Streptomyces venezuelae* which acts by inhibiting peptidyl transferase, reducing protein synthesis. Its toxicity threshold was found to be quite high, >0.85 mM or >275 mg/L. Biotransformation of this pharmaceutical was performed in the Celligen using 160 mg in 6 ml toluene placed in dialysis tubing. After several attempts, the reaction was allowed to proceed for 4 days and the medium was then extracted and analyzed for products. Purification of the crude extract using a chromatotron showed that only starting material was recovered. This may be explained by two theories. First, the main form of metabolism for chloramphenicol *in vivo* is derivatization. That is, it undergoes glucuronidation and is immediately excreted. If this is the case *in vitro*, isolated material which was dismissed as cellular products may have contained the derivatized drug, with no other metabolite production made possible. Second, chloramphenicol is known to have Cyt-P450 inhibitory effects; perhaps this is what prevented *in vitro* metabolism of the drug by Cyt-P450 enzymes (30).

The final pharmaceutical which was chosen for biotransformation was spironolactone. This is used as a diuretic and acts by competitively blocking the binding of aldosterone to its receptor in the distal tubule of the kidney. This was chosen for encapsulated biotransformation due to its water insolubility, and on account of this, a toxicity assay was not performed. Toluene was not chosen since it was feared that partitioning between the organic/aqueous phase would be hindered with the high solubility of the drug for this solvent. The diffusion of the drug between phases largely depends on its partition coefficient. For example, it was found that the partition coefficient for pyrilamine maleate in octanol/water was 3.45:1. Hence, pyrilamine is present in greater amounts in the organic phase when both phases are of equal volume. It was determined that biotransformation time was doubled in the substrate-encapsulated system as opposed to the free cell aqueous system due to this partitioning.

Assuming that the toxicity threshold of spironolactone was approximately 100 mg/L, a greater amount of 162 mg was added to 5 ml of hexadecane in the Celligen which contained 1.3 L of medium/MLC. After 4 days of biotransformation, the medium was collected and extracted. The crude product (127 mg) was collected (small quantities of spironolactone remained in the dialysis tubing due to an unfavorable partition coefficient) and purified. It was determined that one major metabolite, canrenone (structure 4 in experimental

section) was produced in 70% yield. Canrenone is also a major human metabolite of spironolactone. This metabolite is also active as a diuretic agent, contributing to the efficacy of spironolactone. Interestingly, canrenone, but not spironolactone yields carcinogenic epoxides as metabolites, resulting in restricted use of this pharmaceutical.

A possible mechanism for biotransformation is given in scheme 7.



Scheme 7: Mechanism for biotransformation of Spironolactone to Canrenone

Canrenone may arise from the enzyme-catalyzed elimination of the thioacetate group. Base functionalities such as amino groups present on the enzyme abstract the C-6 hydrogen to form a double bond between C-6 and C-7 upon elimination.

3.2 *Rhodococcus rhodochrous* Project

Due to the lengthy time required to obtain substantial amounts of mammalian cells for biotransformation, a bacterial cell line was considered as an alternate for continuation into the investigation of free-cell versus two-phase and encapsulated bioconversions. *Rhodococcus rhodochrous* is known to perform nitrile bioconversions via a two step pathway involving nitrile hydratase (NHase) and amidase (see Figure 8, page 19). The kinetics for the conversion of heptyl nitrile and CPIN to their corresponding acids were investigated in free cell, two-phase and encapsulated systems.

3.2.1 *Optimization of Growth conditions*

Many strains of *Rhodococcus rhodochrous* exist, all of which utilize similar growth medium, but using these strains for nitrile bioconversions requires specific supplements which vary from strain to strain. The nitrile hydratase (NHase) enzyme must be induced for optimal synthesis to occur during cell growth. The presence of an amide/amine containing substrate during growth increases NHase production, the degree of which can vary depending on what substrate is used. In addition, NHase enzymes require a metal cofactor which differs from strain to strain, some of which prefer Co^{2+} , Fe^{3+} , or Fe^{2+} . Some Fe^{3+} containing NHase are light sensitive, and require light irradiation for activation

(see Figure 12). Hence, growth medium characterization of *Rhodococcus rhodochrous* ATCC 17895 was investigated.

Separate flasks of *Rhodococcus* sp. containing 0.1 g/L FeSO_4 , 0.1 g/L CoCl_2 , and 1 g/L caprolactam ($\text{CH}_2(\text{CH}_2)_4\text{CONH}_2$) respectively were cultivated. After 48 hr, it was observed that the flask containing CoCl_2 showed no cell growth. Lower concentrations of CoCl_2 (0.01 g/L and 0.005 g/L) produced the same results. It was concluded that Co^{2+} was not a cofactor requirement but in fact a toxic substance to the cells.

The flasks containing Fe^{3+} and caprolactam, along with a control (which did not contain any Fe^{3+} , Co^{2+} or caprolactam) were harvested and a free cell, two-phase and encapsulated biotransformation of heptyl nitrile were performed. After 48 hr, the media were extracted and analyzed by GC. It was found that trace amounts of octanoic acid were produced in every flask, including the control. In order for better reduction, *Rhodococcus* sp. was grown in a medium which contained both Fe^{3+} and caprolactam, which showed a dramatic increase in the amount of acid produced after 48 hr in a free cell system (no starting material was detected). The amount of Fe^{3+} was reduced to 0.01% (w/v) from 0.1% (w/v) due to aggregation of the capsules caused by excess Fe^{3+} and this reduction caused no difference in the amount of product yield when coupled with caprolactam induction. Reducing the amount of caprolactam by half, however, makes induction of NHase unsuccessful.

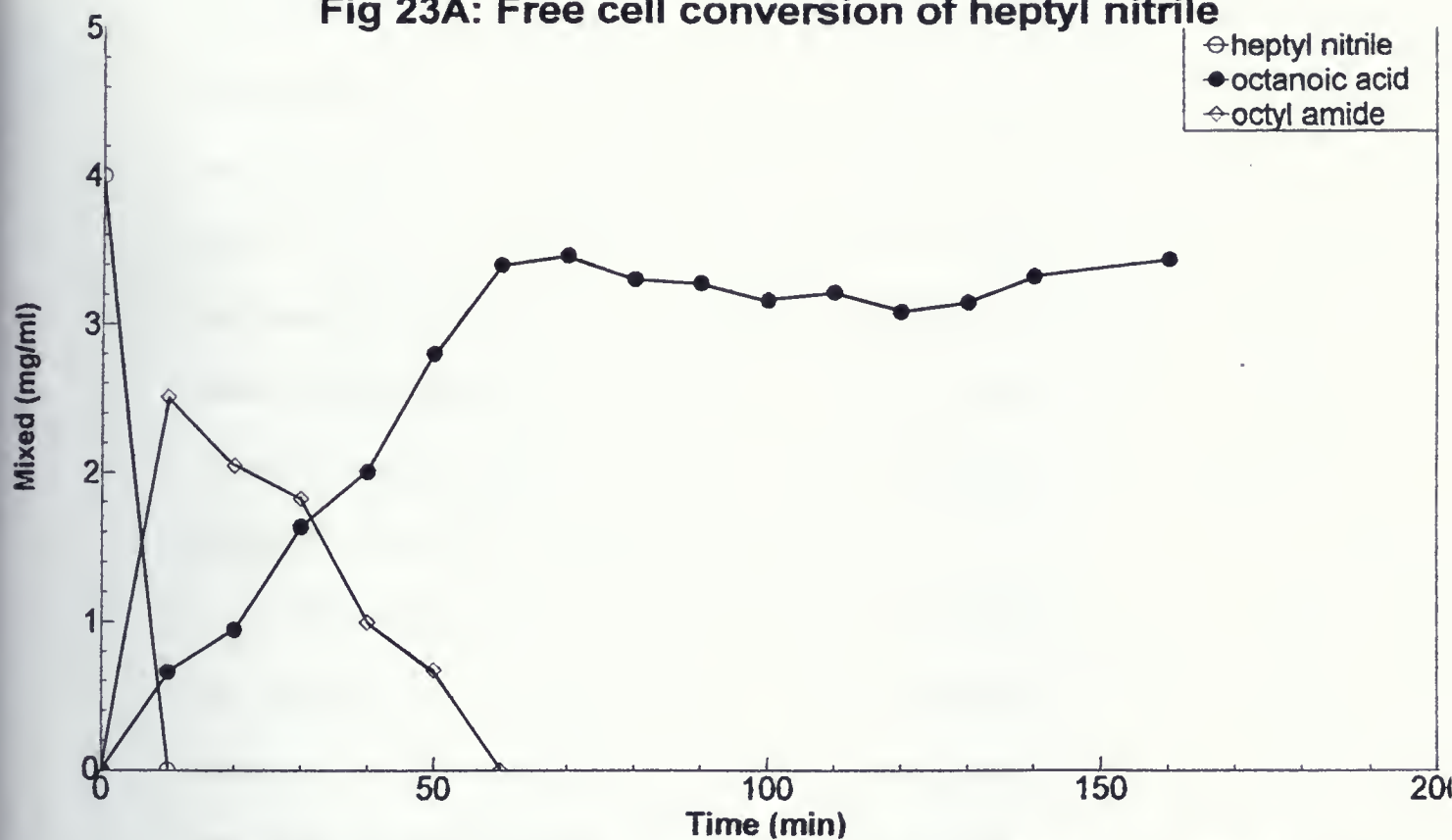
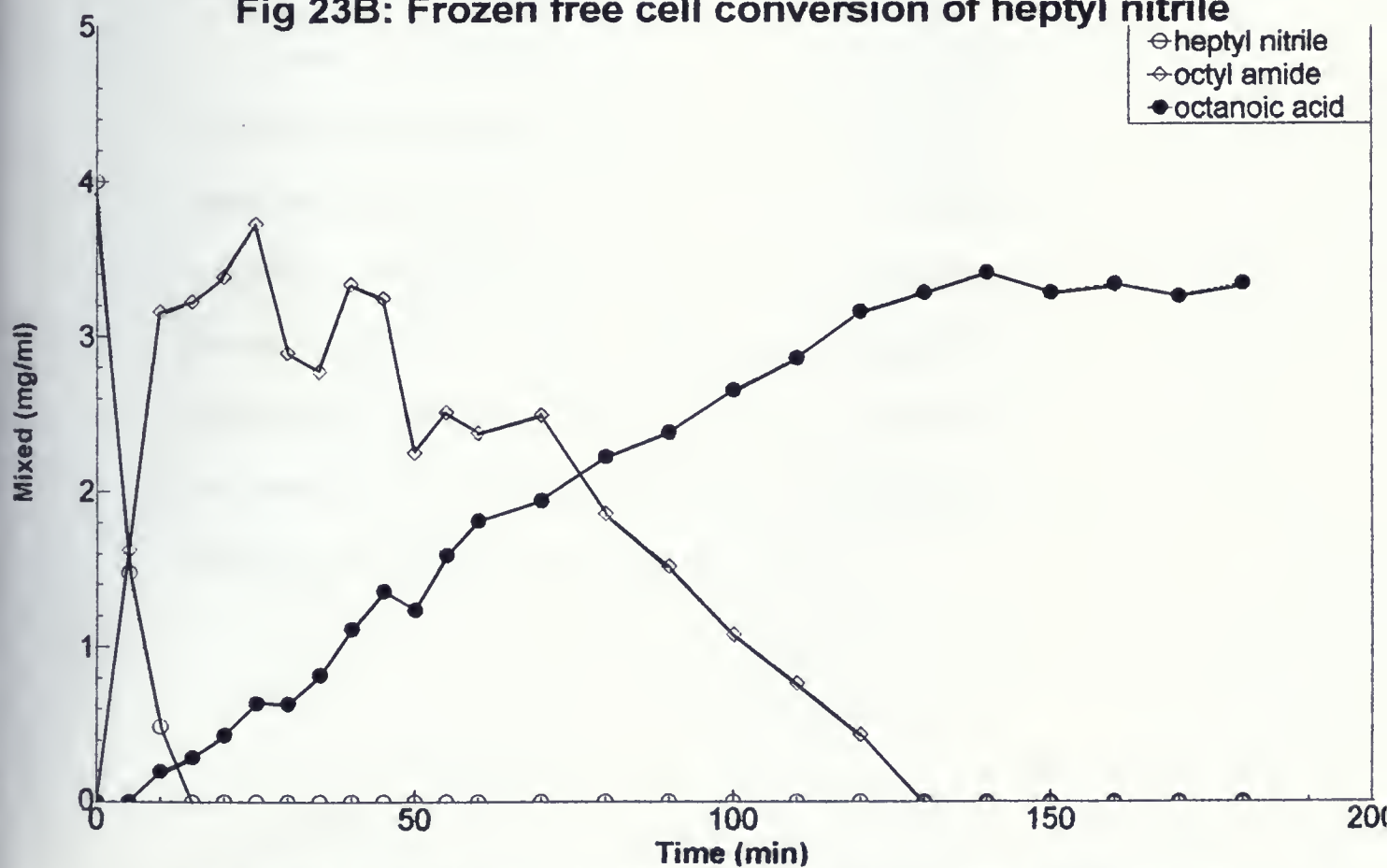
Light sensitivity was investigated by growing the *Rhodococcus* sp. in the presence of 0.01% (w/v) FeSO_4 and 0.1% (w/v) caprolactam in the dark (covered with aluminum foil) and light. Biotransformation of heptyl nitrile by these cells showed no difference in the rate/amount of product produced. Hence this strain of *Rhodococcus* sp. does not possess light induced enhancement of its nitrile hydratase enzyme.

Temperature sensitivity experiments showed that the nitrile hydratase was functional to the same degree (as measured by conversion of nitrile to product) between the temperatures tested of 25-35 °C. The amidase enzyme, however, seemed to function slightly faster (as measured by the disappearance of amide intermediate) at higher temperatures of 32-35 °C.

3.2.2 Heptyl Nitrile Biotransformation

Free Cell

A time study was performed for the free cell bioconversion of heptyl nitrile in which samples were taken every 10 min. In doing so, an amide intermediate, previously undetected, was observed. The time course is shown in Figure 23 A. From this graph, it is evident that heptyl nitrile is converted to 100% amide in less than 10 min. Once the amide has formed, acid production is observed. The amide species is depleted until complete conversion to acid occurs in 60min. Verification that this was an amide intermediate was given

Fig 23A: Free cell conversion of heptyl nitrile**Fig 23B: Frozen free cell conversion of heptyl nitrile**

**** Biotransformations performed with a cell concentration of 100mg/ml wet weight**

when a standard of synthesized octyl amide spiked and identified the amide peak during GC analysis. Octyl amide itself was also fed to *Rhodococcus* sp. and found to be transformed to octanoic acid (octanoic acid was identified in the same manner as the amide intermediate). In addition, control samples of heptyl nitrile, octyl amide and octanoic acid were placed separately in Tris buffer, pH 7.2 and monitored daily by GC. Auto hydrolysis of these compounds was not observed in the absence of *Rhodococcus* sp. cells.

Cells of *Rhodococcus* sp. were harvested and put in the freezer for a period of 1 week in order to determine whether the enzymes would remain viable, and if so, the *Rhodococcus* sp. cells could be stored in this manner. A time study for a free cell biotransformation of heptyl nitrile was carried out.

Referring to Figure 23 B, it is evident that the enzymes survived freezing. It is interesting to note that the NHase functioned just as rapidly converting the nitrile substrate to 100% amide within 15min. The amidase enzyme, however, appears to be less efficient in converting the amide intermediate to acid, taking 130min as opposed to 60min. Thus, for purposes of isolating the amide intermediate, freezing the cells is advantageous, and in addition, for monitoring the kinetics of the two-phase reaction, the amide intermediate would have more of a chance to sequester in one of the two phases.

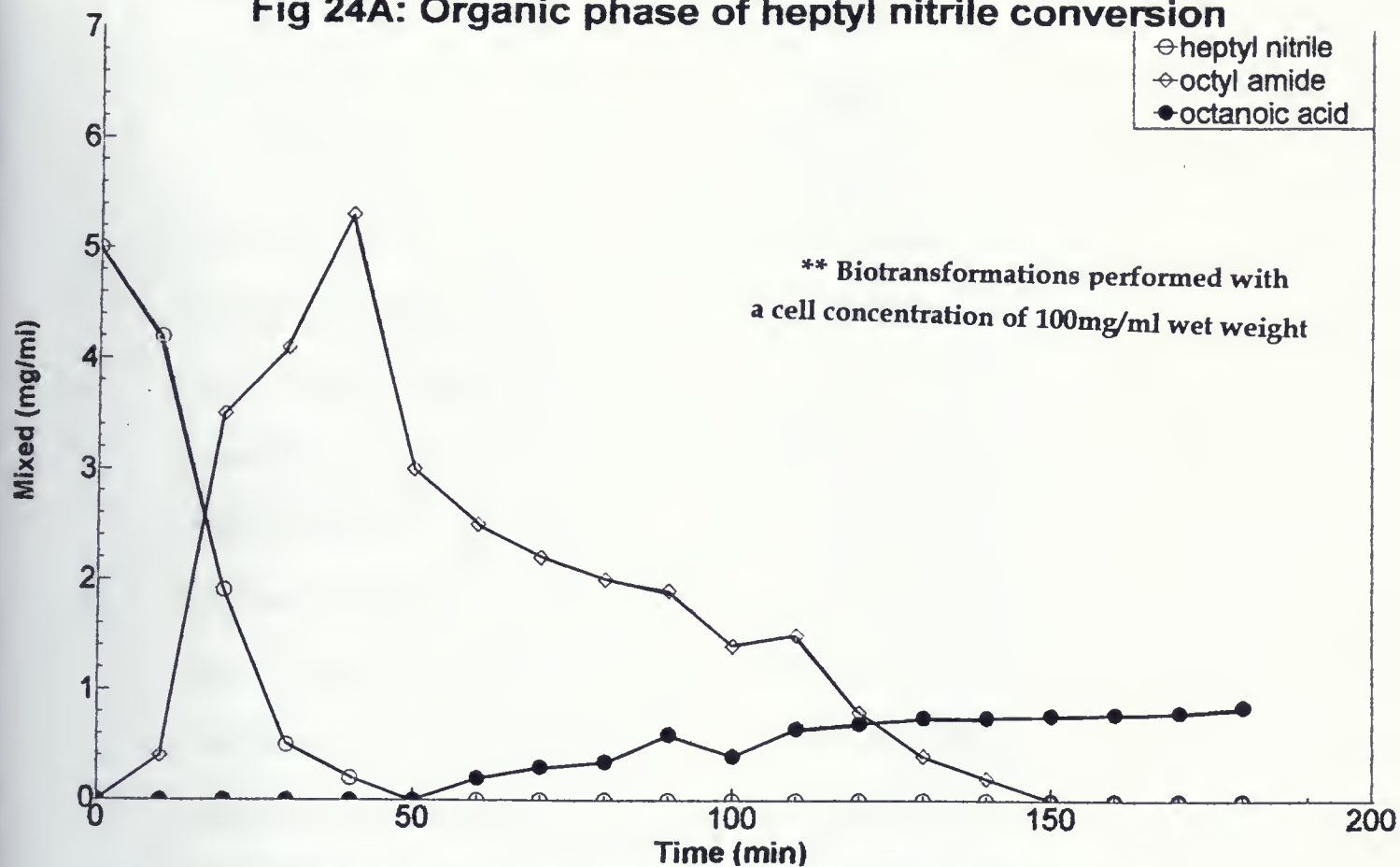
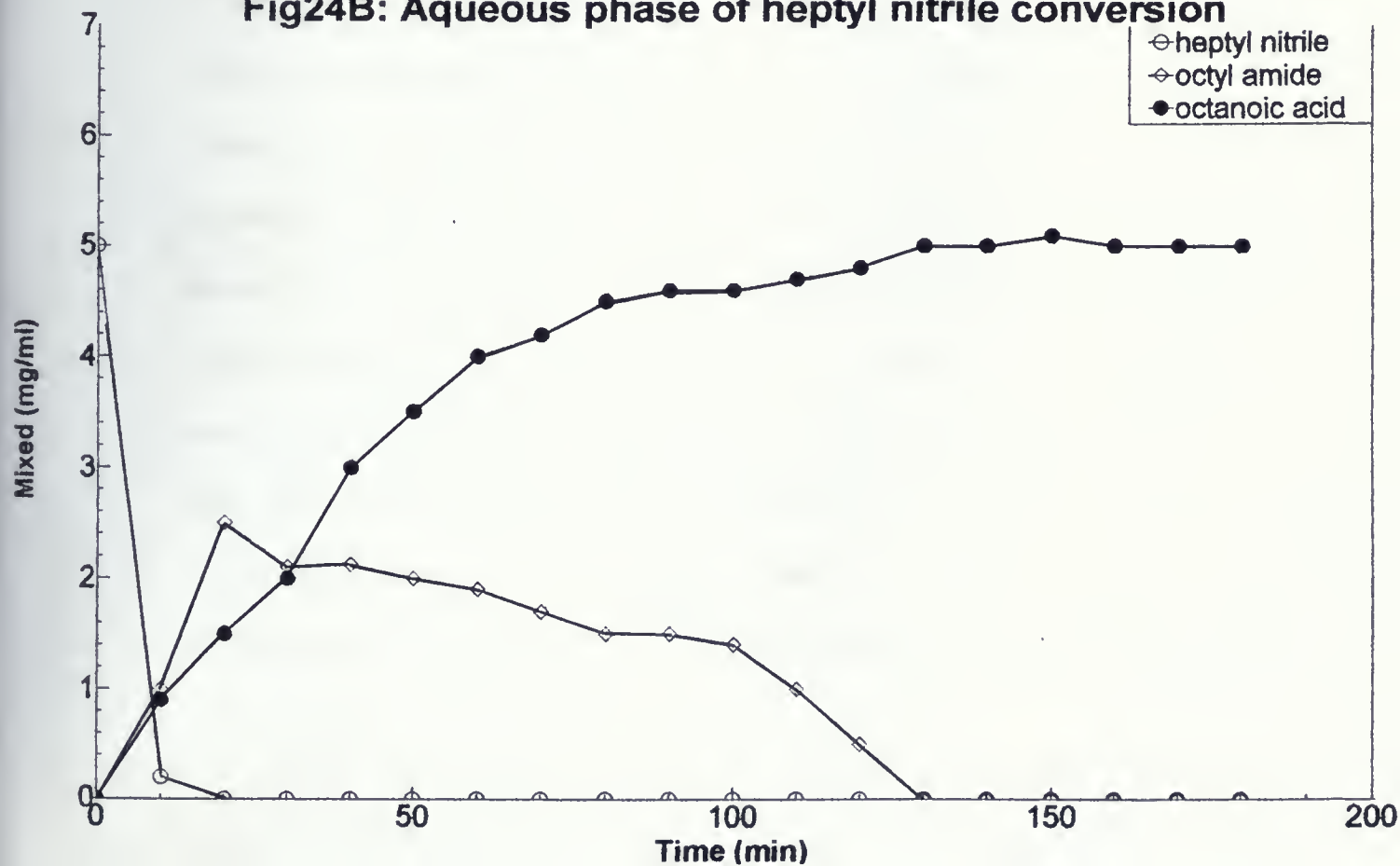
Two-phase

A two-phase biotransformation was performed to investigate whether the amide intermediate could be trapped in one of the phases apart from its acid product. A 50:50 ratio of 0.5 M Tris buffer, pH 7.2 and octane was used for this system. Emulsification of the two phases did not occur during biotransformation (reaction was placed on a shaker at 180 rpm), making it possible to take samples from both phases for the kinetic studies.

Referring to Figure 24 A and B, the amide appears to have stayed primarily in the organic phase (A), whereas the acid persists in the aqueous phase (B). This was expected since at pH 7.2, the acid exists mainly in its ionized form, and the amide, having a higher pKa value exists in its un-ionized form. This analytical system has proven to be successful for monitoring the disappearance of substrate and the formation of products. In addition, it has illustrated that *Rhodococcus* sp. can perform nitrile hydrolysis in a two-phase environment.

Encapsulated

Rhodococcus sp. cells have a low tolerance for MOPS buffer, with viability lasting only a few hours in its presence even in concentrations as low as 0.3 M (3). Tris and phosphate buffers were examined for their toxicity to the cells and found to be nontoxic at 0.5 M concentrations. The acid chloride:PAA ratio of 1:1 was restored since the bacterial cells show a higher resistance to damage from

Fig 24A: Organic phase of heptyl nitrile conversion**Fig24B: Aqueous phase of heptyl nitrile conversion**

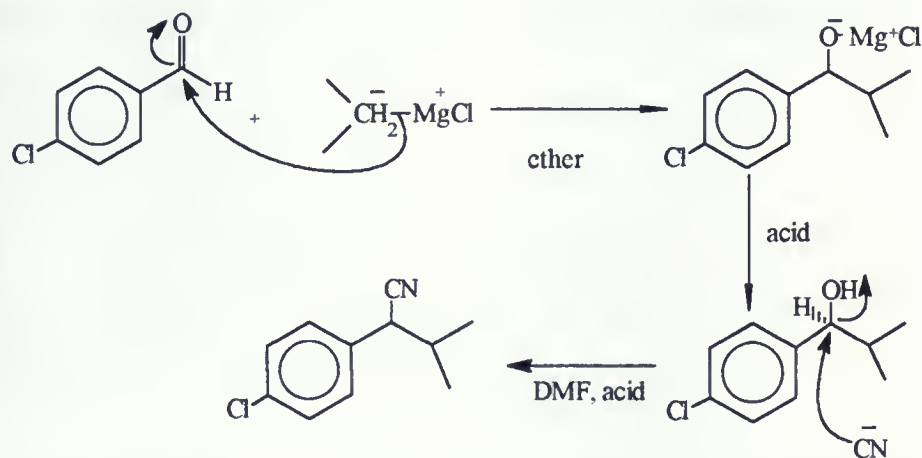
the acid chloride. All other conditions remained in accordance with the procedure developed by Khan *et al.* (7). The capsules produced using Tris and phosphate buffers were not particularly stable since the *Rhodococcus* sp. cells had a tendency to remain at the interface of the droplets, rather than within them (see Figure 1 for schematic). Thus, upon polymerization at the interface, the cells interfered and caused leaky membrane formation. Encapsulation using MOPS buffer produced excellent beads, since the cells remained within the aqueous droplets, but viability was reduced to 50% (3). Bioconversions of heptyl nitrile with Tris encapsulated *Rhodococcus* sp. produced trace amounts of acid after 3 hr. However, the possibility that free cells performed the conversion is likely since capsule leakage occurred. Auto hydrolysis does not appear to be a viable answer to the production of octanoic acid since it was not evident in control flasks containing heptyl nitrile in Tris buffer pH 7.2, in the absence of cells over time. Octyl amide was not detected in the bulk organic phase or within the capsules themselves, but since conversion to acid was so rapid in the free cell system, it was not surprising. Biotransformation using the MOPS encapsulated cells showed no conversion at all after repeated attempts. Viability of the encapsulated cells was difficult to assess by inoculating disrupted capsules onto agar plates due to the capsular debris present. Subculturing these plates, however, showed no viable growth. Hence, further time studies on encapsulated systems was halted. Time constraints prevented further work.

3.2.3 CPIN Biotransformation

2-(4-chlorophenyl)-3 methylbutyronitrile, or CPIN as abbreviated, is produced industrially as a pesticide, its amide counterpart, however, has potential medicinally as an anti-inflammatory agent. Both compounds are unavailable commercially, making it necessary to synthesize CPIN. Biotransformation of this starting material was shown to yield the amide and acid products.

Synthesis of CPIN

The first approach to synthesis of CPIN was to perform a Grignard reaction using 4-chlorobenzaldehyde and isopropylmagnesium chloride. The mechanism is given in scheme 8.



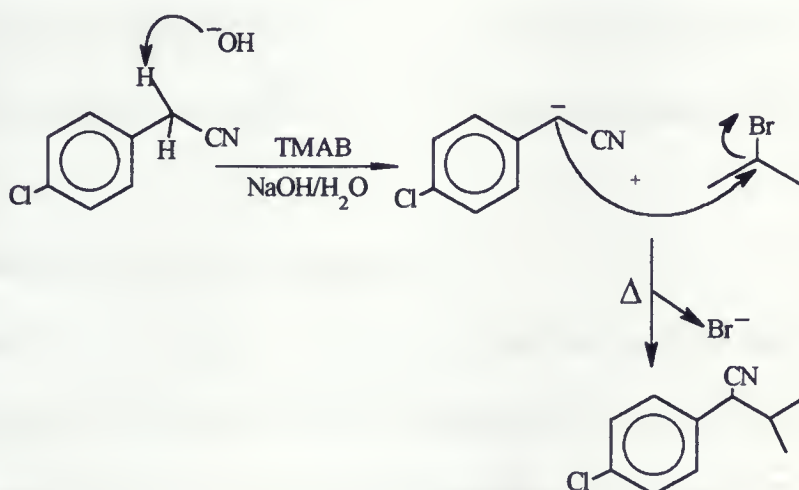
Scheme 8: Mechanism for synthesis of CPIN using Grignard Reaction
DMF: dimethylformamide, CN^- is from treatment with KCN

The first step of this synthesis involves the nucleophilic attack of isopropyl magnesium chloride which acts as a carbanion, on the carbonyl of the

chlorobenzaldehyde, forming an oxyanion intermediate. Addition of acid breaks up the interaction of the oxyanion with the magnesium chloride complex and forms a secondary alcohol. The secondary alcohol is then converted to the nitrile via a substitution reaction, with the leaving group being water. Crude NMR analysis of the first step, revealed very low yield of alcohol, with other side-products apparent (were not identified). It was speculated that the Grignard reagent was also interacting with the chlorine substituent on the benzene ring, causing *para* substitution of the isopropyl functionality.

Synthesis using benzaldehyde instead of 4-chlorobenzaldehyde also gave low yields (unoptimized), and progression to the next step was not performed.

At this point, the industrial approach to synthesizing CPIN was performed instead, due to its one step design (32). The mechanism is given in scheme 9.



Scheme 9: Synthesis of CPIN using industrial approach

The use of tetramethylammonium bromide (TMAB) is imperative for the success of this two-phase reaction. 2-bromopropane is immiscible in water, the TMAB functions as a phase transfer catalyst which brings this organic layer into contact with the aqueous, chlorobenzyl cyanide containing layer. Addition of 4-chlorobenzyl cyanide to concentrated base causes the removal of the acidic proton α to the nitrile group. The nucleophilic carbon attacks the bromo substituted carbon of 2-bromopropane through an S_N2 mechanism. The expelled bromine ion forms a white NaBr salt during the course of the reaction.

The reaction gave 80% yield (unoptimized) of CPIN product. Purification via silica gel chromatography was performed to separate unreacted starting materials from the product.

Synthesis of 2-(4-chlorophenyl) methylbutyric acid (CPIN acid) from CPIN was performed by treatment of CPIN with strong base under reflux. After a period of 5 days, 30% CPIN acid was obtained along with 30% CPIN amide. These were separated and used as racemic standards for chiral GC analysis.

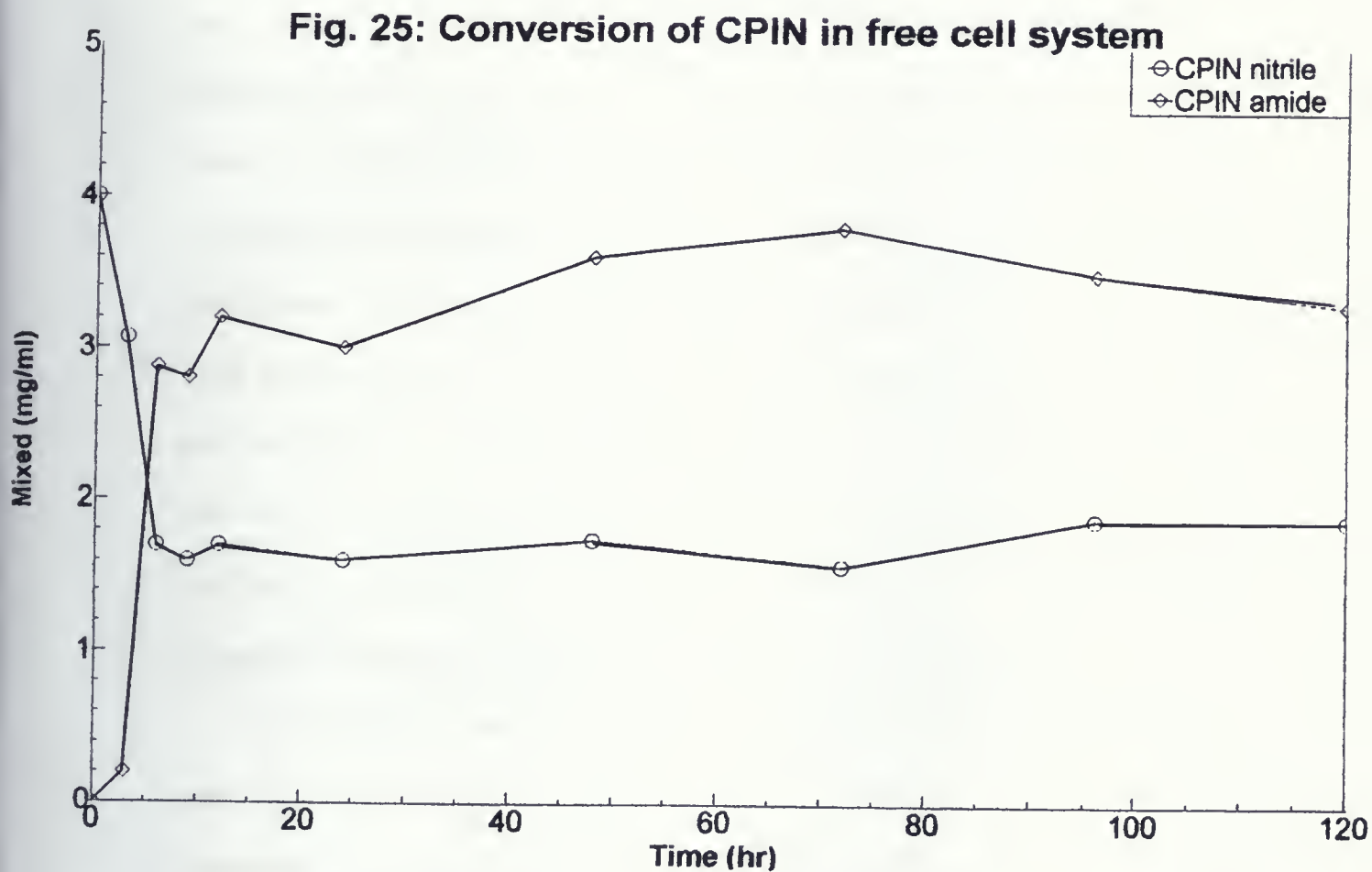
Aqueous Phase Free Cell Biotransformation

Analysis by GC showed that the initial free cell biotransformation of CPIN by *Rhodococcus* sp. was converted to the amide with trace amounts of acid being produced (Figure 25). The crude products were separated, purified and characterized.

Evidence for amide production was obtained by ^1H -NMR, mass spectroscopy and IR. ^1H -NMR showed two identical broad peaks at δ 5.51 and 5.70, suggesting the presence of hydrogen atoms from a nitrogen source. This did not rule out, however, the possibility that the broad peaks may be due to the presence of a hydroxyl group coming from an acid. Mass spectroscopy gave a molecular ion of 211, characteristic of the amide product, however, the molecular weight of the amide differs by only one mass unit from the acid product (212). Repetitive mass units of 14 were also observed to be lost in the mass spectrum, indicative of a nitrogen or CH_2 containing species. IR analysis confirmed the presence of an amide functionality, with peaks at 3200 and 3350 cm^{-1} . A large broad peak was not observed, eliminating the possibility of an acid functionality being present in this fraction of pure sample.

CPIN acid was identified by ^1H -NMR, ^{13}C -NMR, MS and IR. A downfield shift was observed for the hydrogen atom α to the carbonyl functionality when compared to the CPIN amide hydrogen atom in ^1H -NMR. In addition, the two broad peaks observed for the amide hydrogens were not seen in the CPIN acid spectrum. ^{13}C -NMR comparison between the products showed a small downfield shift in the carbonyl carbon, with all other peaks remaining the same. Mass spectrometry analysis resulted in a molecular ion species of 212. These results, in conjunction with IR analysis which showed a single broad peak at 3000 cm^{-1} confirmed the identity of the product as CPIN acid.

Referring to Figure 25, conversion of CPIN in a free cell system lead to approximately 40% conversion to its amide, over a period of 10 hr whereupon the reaction appeared to slow down. Problems with CPIN solubility in water were encountered, and dissolving the substrate in ethanol before addition to the *Rhodococcus* sp. cells did not improve its solubility. Hence, conversion to the amide was limited by the amount of CPIN which dissolved in the aqueous buffer. In addition, the amidase enzyme may be inhibited by the presence of excess nitrile compound. Furthermore, CPIN amide may not be a suitable substrate for the amidase due to the steric hindrance provided by the isopropyl functionality. Trace amounts of acid production were observed, but may be due to auto hydrolysis, since this was evident in the control sample containing CPIN amide in Tris buffer, pH 7.2 in the absence of *Rhodococcus* sp. In the control, minute amounts of CPIN amide were converted to CPIN acid within minutes, but the levels of CPIN acid did not increase further over time. The control sample containing CPIN, remained inert over 7 days, with no CPIN amide or CPIN acid being detected. The viability of *Rhodococcus* sp. during biotransformation was tested by inoculating samples onto agar plates after each day of biotransformation. It was found that the cells remained viable for a period of 4 days in the free cell environment.

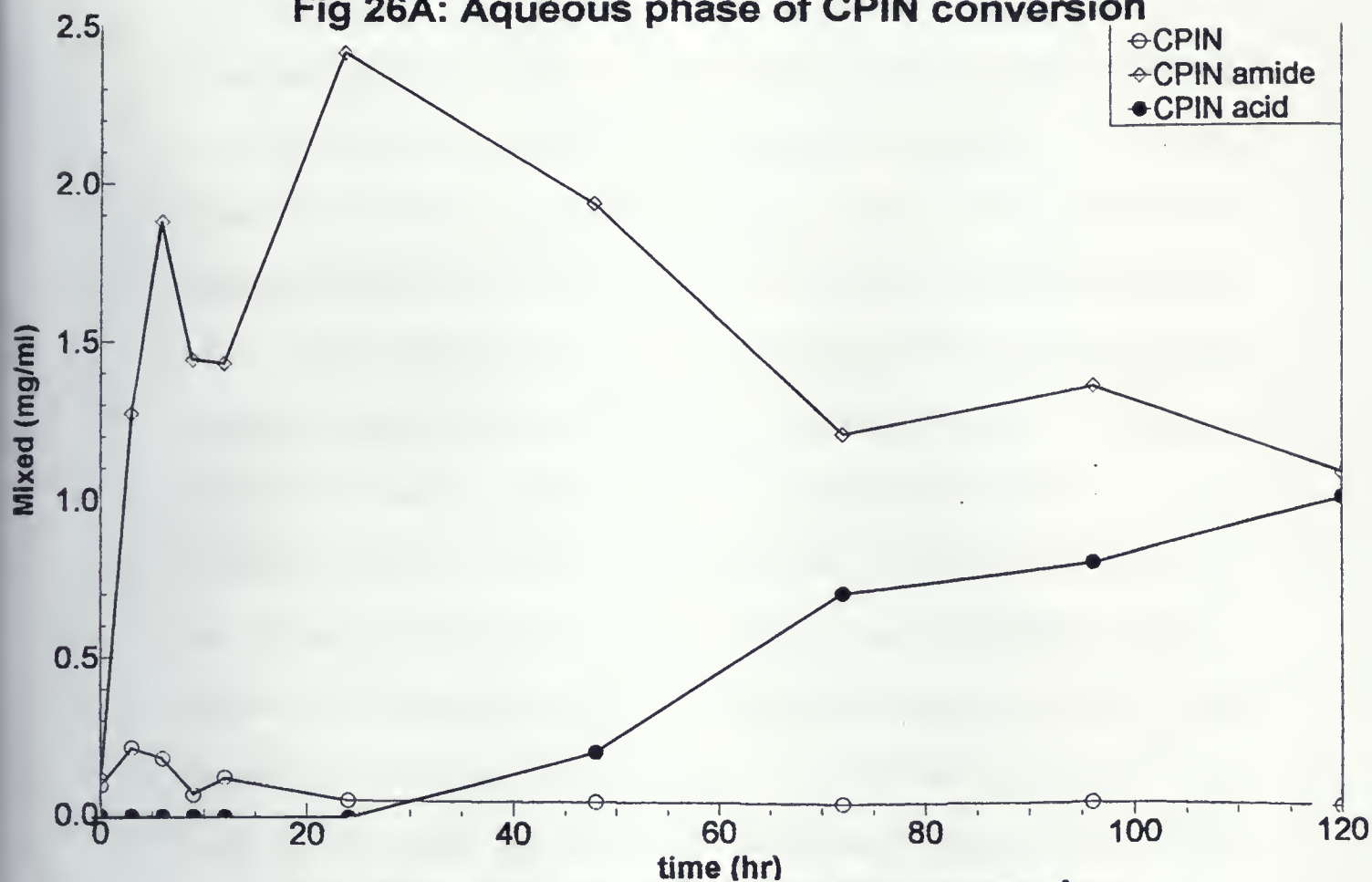
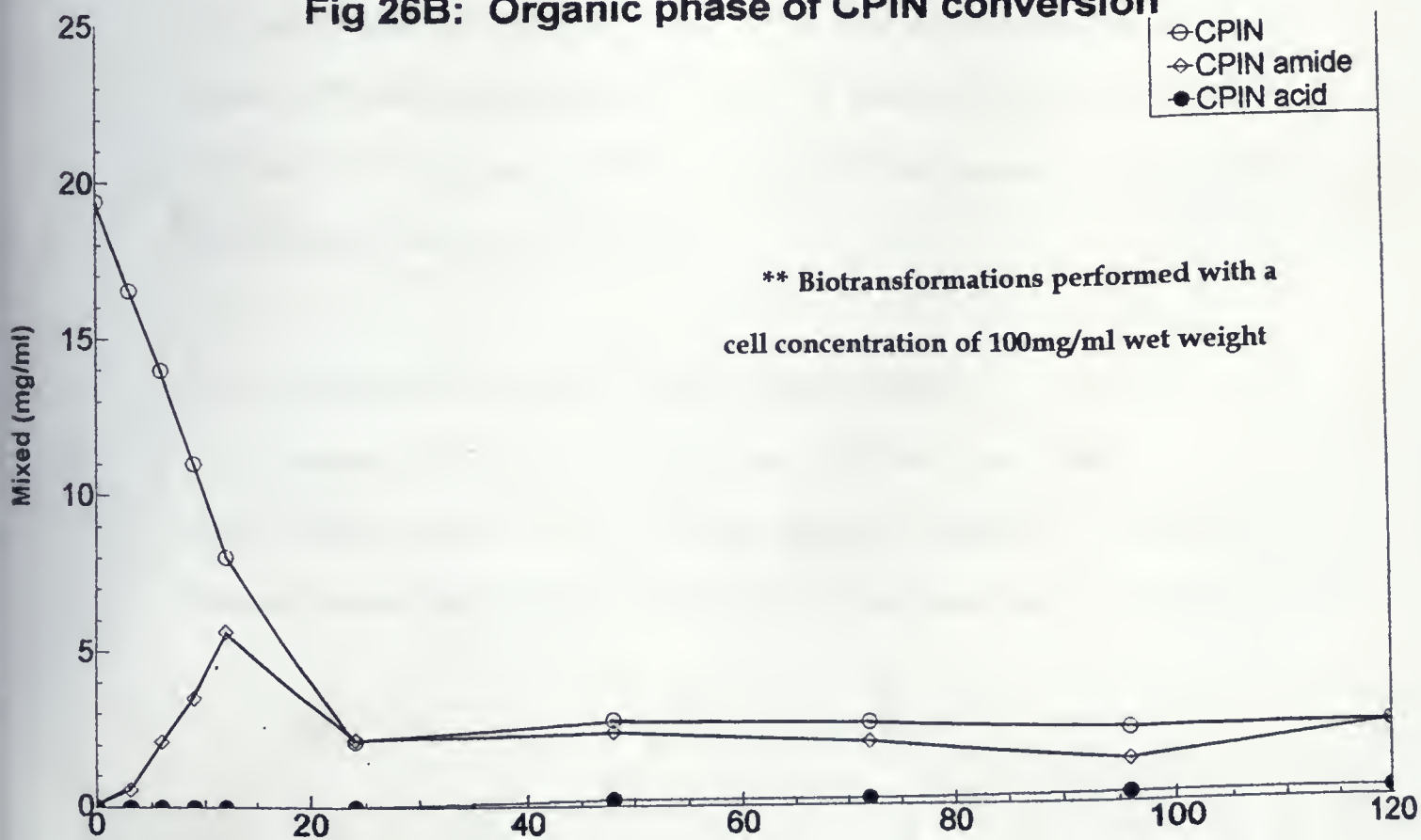


**** Biotransformations performed with a cell concentration of 100mg/ml wet weight**

Two-Phase Biotransformation

A 50:50 aqueous:organic mixture of Tris buffer and octane were used as the medium for two-phase biotransformation of CPIN. Preliminary studies revealed that only a small amount of amide/acid was being produced with the majority of CPIN remaining in the organic phase. It appeared that the solubility of CPIN was far greater in the organic phase, making it difficult for transfer to the aqueous. Investigation into the partition coefficient of CPIN was performed with various solvents such as octane, heptane, hexane, toluene, ethylacetate, dichloromethane and chloroform. A 50:50 mixture of the solvent with tris buffer and a known amount of CPIN were analyzed (organic phase only) by GC before and after 24 hr of mixing. In all cases, the concentration of CPIN remained constant, suggesting that the partition coefficient is extremely high.

Two-phase systems with a 2.5:1 and 5:1 ratio between Tris buffer pH 7.2, and octane layers, respectively, were performed to try and increase CPIN partitioning into the aqueous phase. Preliminary studies showed an increased amount of amide and acid being produced for both ratios of aqueous:organic. The 5:1 ratio was chosen for ease of sampling from the organic octane phase (due to larger volume). Referring to Figures 26 A and B, the amide was present in both the aqueous and organic phases whereas the acid was observed in the aqueous phase, with CPIN in the organic layer. Emulsification of the cells in the organic

Fig 26A: Aqueous phase of CPIN conversion**Fig 26B: Organic phase of CPIN conversion**

phase occurred after 2 days, making sampling of this phase difficult, but the general trend for product formation was obtained upon graphing. The aqueous phase revealed that the reaction did not produce as high a yield as the free cell biotransformation (30% as opposed to 40%), but the extent of conversion of CPIN amide to CPIN acid was greatly increased, with 95% of the CPIN amide produced being converted to CPIN acid after 2 weeks (data point not shown on graph). This was not apparent in the free cell system which contained mainly CPIN amide after two weeks. The viability of the cells in the two-phase system was difficult to determine due to emulsification and the presence of organic solvents on the agar plates. Cells were observed to be viable for up to 2 days during biotransformation on the agar plates, but upon emulsification of the cells in the organic phase, cell plating was inconclusive. The membrane bound amidase enzyme continued to remain active after this time period, however, since CPIN acid production persisted over 2 weeks. The higher activity of amidase in the two-phase system may be due to the removal of excess CPIN which remained in the organic phase.

3.2.4 Chiral analysis of CPIN biotransformation products

Samples of CPIN, CPIN amide and CPIN acid were taken at various stages of free cell and two-phase biotransformation. Samples were analyzed by chiral GC as specified in section 2.2.9. Chirality of the compounds showed no

difference between free cell and two-phase biotransformations. Referring to Table 10, CPIN remained virtually racemic through the time study, suggesting that the nitrile hydratase enzyme in *Rhodococcus rhodochrous* ATCC 17895 is not specific for a single enantiomer, since the CPIN racemate was converted to the amide.

Table 10: Results of chiral analysis of CPIN and products

Time interval	CPIN	CPIN amide	CPIN acid
2 days	racemic	12.6%	----
9 days	----	94.3%	----
14 days	----	51.6% (rev)	97.3%

Rev: A reversal of enantiomeric purity was observed

Looking at Figure 27A, CPIN amide showed increasing enrichment of enantiomer 2 and a reduction of enantiomer 1 over a period of 9 days. After 9 days, the enantiomer 2 peak was reduced in area and the residual enantiomer 1 peak became enhanced with an ee of 51.6% after 14 days. It can be said that the amidase enzyme of *Rhodococcus rhodochrous* ATCC 17895 shows high selectivity for enantiomer 1 of CPIN amide since 97.3% ee was obtained for CPIN acid after 14 days (Figure 27B). The reversal of ee for CPIN amide after 14 days may be explained by the introduction of a late induced enzyme in the whole cell system capable of using the amide as a substrate for its metabolism. The enzyme may appear after the culture has aged for a period of time, and preference for the

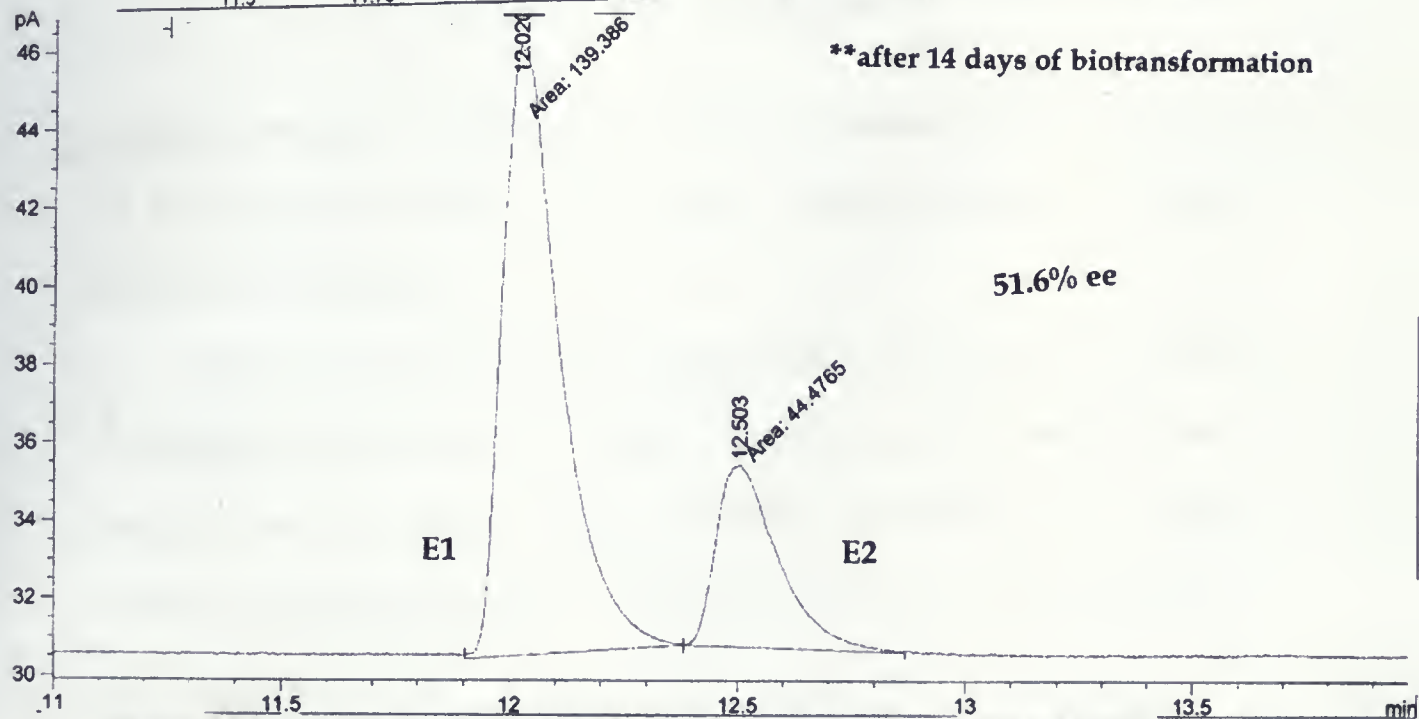
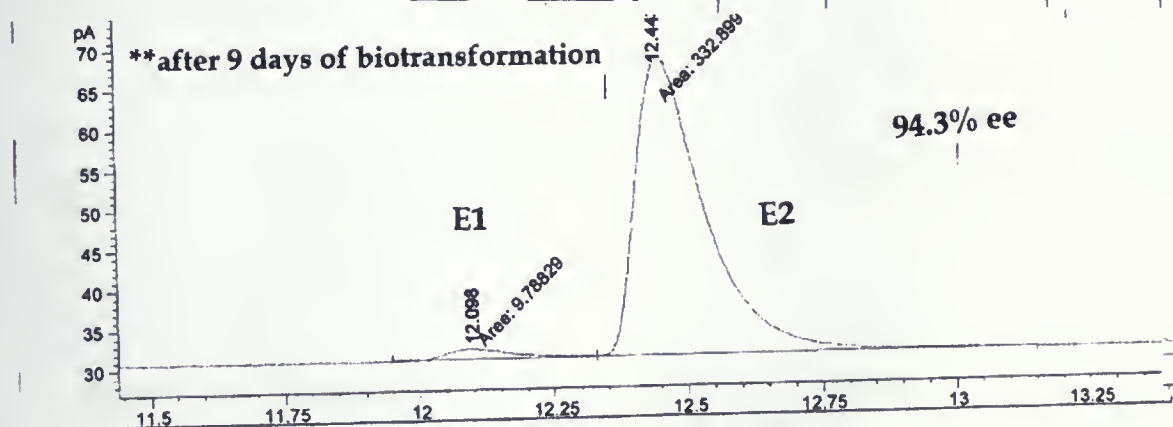
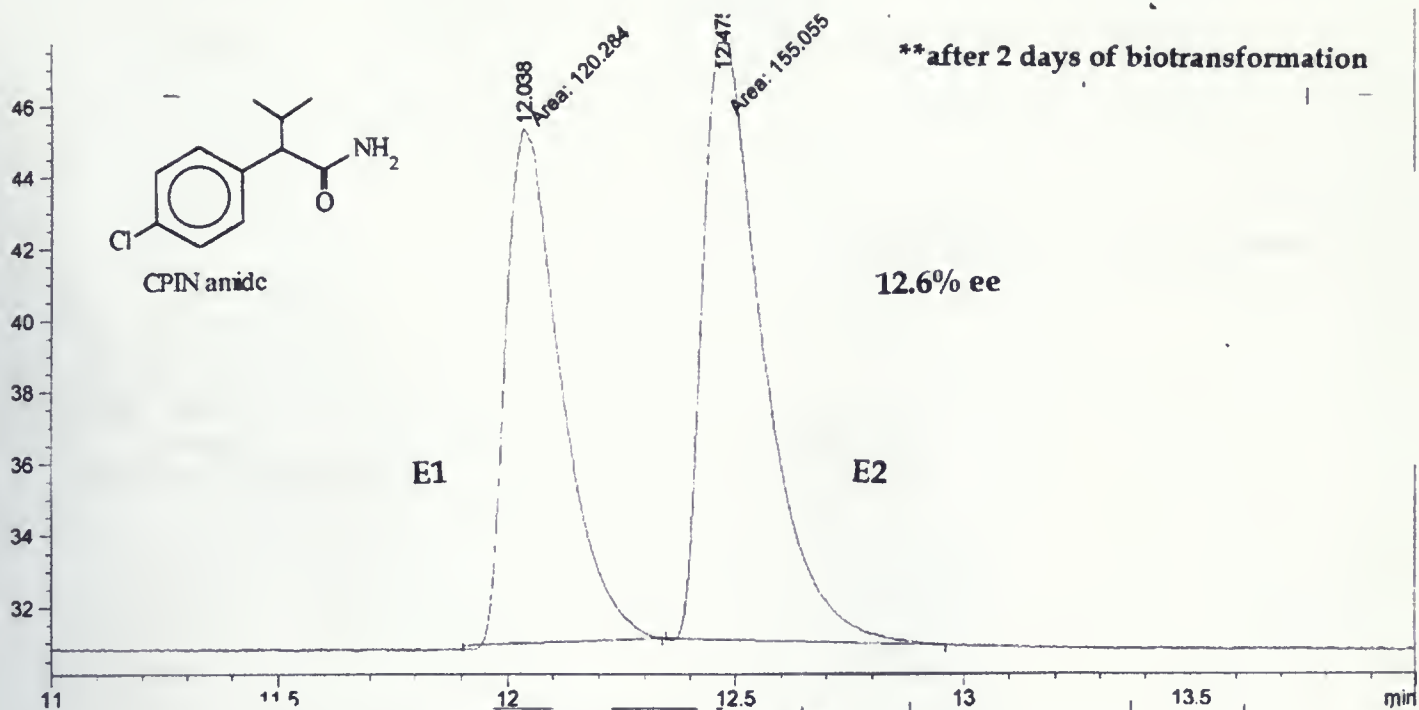


Figure 27A: Enantiomeric peaks obtained upon chiral analysis of CPIN amide

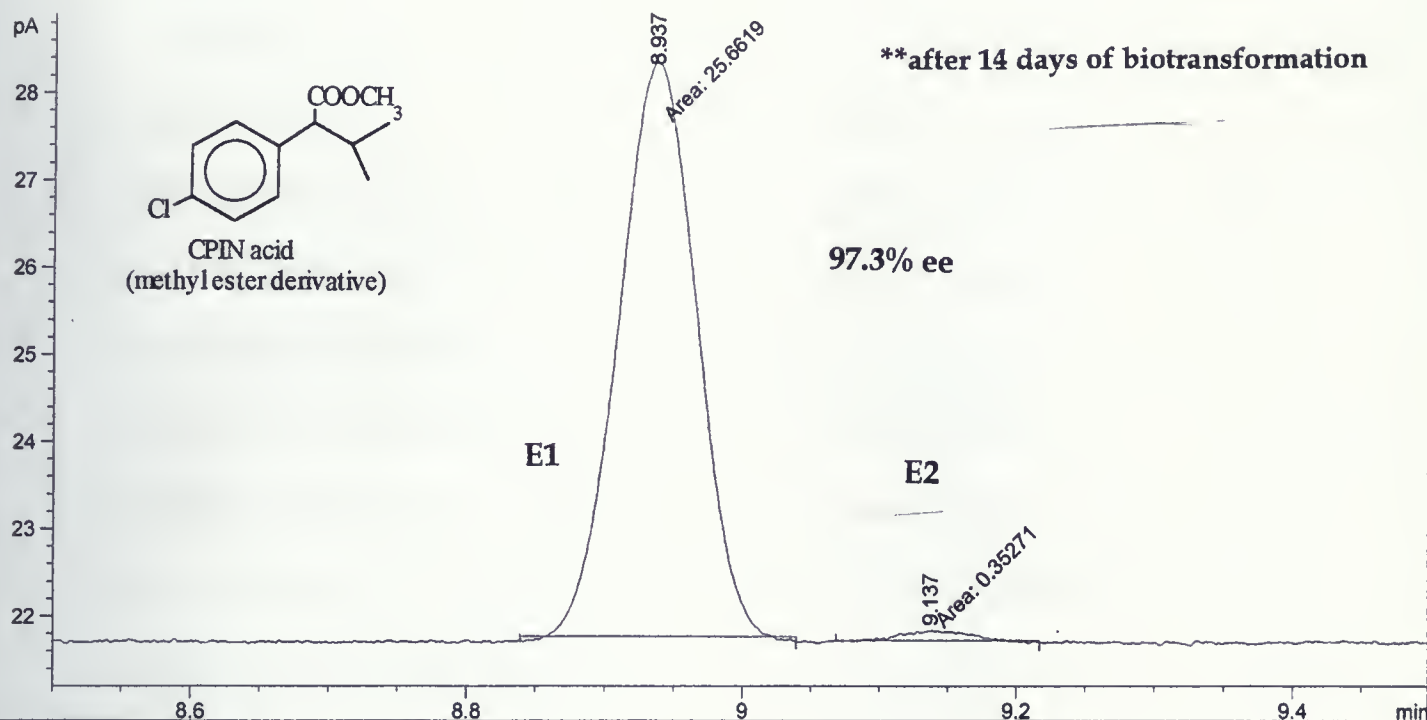


Figure 27B: Enantiomeric analysis of CPIN acid in ester form after 14 days of biotransformation

opposite enantiomer to the amidase is shown. The amidase enzyme itself could not have metabolized both enantiomers since a reduction in ee for CPIN acid would have been observed.

The identity of the enantiomers obtained (*R* or *S*) was not possible since enantiomeric standards were not available. The common theme in the literature (24, 25) is that the amidase enzyme has strict *S*-selectivity for CPIN amide whereas the nitrile hydratase may possess poor selectivity for the *S* enantiomer

of CPIN. The latter was not observed in this case. The advantage of having non-selectivity in the nitrile hydratase enzyme is that higher yields of enantiomerically pure CPIN amide and CPIN acid are attainable. Fallon *et al.* (25) explored a *Pseudomonas* sp. which had no amidase activity which is useful, if CPIN amide is solely desired since purification is simplified. *Rhodococcus rhodochrous* ATCC 17895 has the ability to produce enantiomerically rich CPIN amide a free cell conversion and enantiomerically rich CPIN acid in a two phase system. *Pseudomonas* sp. does not have amidase activity and a high tolerance for organic solvents like *Rhodococcus* sp., making CPIN acid formation and a two-phase system biotransformation unlikely.

Conclusions and Future Work

In conclusion, encapsulation of mammalian cells using interfacial polymerization and polyallylamide capsules proved unsuccessful. Perhaps applying the sol-gel method of encapsulation (see Peterson *et al.* (11), page 10) would prove to be fruitful since it has been performed on mammalian cells for aqueous environments and applications of lipase containing sol-gel beads in organic solvents has also been performed. Investigation into organic solvent permeation of the sol-gel beads would uncover the feasibility of this idea.

The reverse capsules which were prepared were not stable enough for practical use but the application of dialysis tubing for substrate encapsulation has potential in the biotransformation of water insoluble compounds by mammalian cells. Future work could involve engineering a two-phase bioreactor based on the dialysis tubing principle.

Encapsulation of *Rhodococcus rhodochrous* did not provide any advantage since cell viability was poor due to the toxicity of MOPS buffer. In addition, phosphate and tris buffers did not allow for stable capsule formation. Screening of other physiological buffers which would not interfere with the polymerization process during capsular formation and prove not to be toxic to the cells is required.

Free cell conversion of CPIN by *Rhodococcus rhodochrous* produced CPIN amide in 40% yield and 94% ee, which is an improvement on the chemical process which gives racemic CPIN amide and CPIN acid in 30% yield. CPIN acid production was enhanced in the two-phase system with 30% yield and 97% ee obtained. If increased yields of product and shorter conversion times were possible, then a continuous two-phase process may be possible. The characterization of the CPIN amide and CPIN acid enantiomers produced must also be performed.

References

1. Yamada, H., Kobayashi, M. Nitrile Hydratase and its applications to industrial production of acrylamide. *Biosci. Biotech. Biochem.* **60**: 1391-1800, 1996.
2. Lee, I.Y., Volm, T.G., Rosazza, J.P.N. Decarboxylation of feurulic acid to 4-unylguaicol by *Bacillus pumulus* in aqueous/organic solvent 2-phase system. *Enzyme Microb. Technol.* **23**: 261-266, 1998.
3. Holland, H.L., Riffle, D., Gu, J.X. Encapsulated Biocatalysts for organic transformations. Pg 128-133.
4. Manosroi, J., Sripalakit, P., Manosroi, A. Bioconversion of hydrocortizone to a predisolone by immobilized bacterial cells in a two-liquid phase system. *J. Chem. Tech. Biotech.* **73**: 203-210, 1998.
5. B., Simon. *Microencapsulation: Methods and Industrial Applications*, Marcel Dekker Inc., USA, 1996.
6. Chang, T.M.S. Semipermeable Microcapsules, *Science* **146**: 524-525, 1964.
7. Green, K.D., Gill, I.S., Khan, J.A., Vulfson, E.N. Microencapsulation of Yeast Cells and their use as a biocatalyst in organic solvents. *Biotechnol. Bioeng.* **49**: 535-543, 1996
8. Chang, H., Seong, G., Yoo, I., Park, J., Seo, J. Microencapsulation of Recombinant *Saccharomyces cerevisiae* cells with invertase activity in Liquid-core Alginate Capsules. *Biotechnol. Bioeng.* **51**: 157-162, 1996.
9. Wang, T., Lacik, I., Brissova, M., Anilkumar, V., Prokop, A., Hunkeler, D., Green, R., Shahrokhi, K., Powers, A. An encapsulation system for the immunoisolation of pancreatic islets. *Nature Biotechnol.* **15**: 358-362, 1997.
10. Dawson, R.M., Broughton, R.L., Stevenson, W.T.R., Sefton, M.V. Microencapsulation of CHO cells in a hydroxyethyl methacrylate-methyl methacrylate copolymer. *Proc. Soc. Exp. Biol. Med.* **115**: 200-206, 1987.
11. Peterson, K.P., Peterson, C.M., Pope, E.J.A. Silica sol-gel encapsulation of pancreatic islets. *Proc. Soc. Exp. Biol. Med.* **248**: 365-369, 1998.

-
12. Reetz, M.T. Entrapment of biocatalysts in hydrophobic sol-gel materials for use in organic chemistry. *Adv. Mat.* **9**: 943-954, 1997.
 13. Ariga, O., Toyofuku, H., Minegushi, I., Hatton, T., Sano, Y., Nagura, M. Efficient Production of recombinant enzymes using PVA-encapsulated bacteria. *J. Ferment. Bioeng.* **84**: 553-557, 1997.
 14. Bauer, A, Layh, N., Syltatk, C., Willetts, A. Polyvinyl alcohol-immobilised whole cell preparations for the biotransformation of nitriles. *Biotechnol. Lett.* **18**: 343-348, 1996.
 15. Willetts, A., Layh, N. Enzymatic nitrile hydrolysis in low water systems. *Biotechnol. Lett.* **20**: 329-331, 1998.
 16. Kakeya, H., Sakai, N., Sugai, T., Ohta, H. Microbial Hydrolysis as a potent method for the preparation of optically active nitriles, amides and carboxylic acids. *Tetrahedron Lett.* **32**: 1343-1346, 1991.
 17. Sugai, T., Yamazaki, T., Yokoyama, M., Ohta, H. Biocatalysis in organic synthesis: The use of nitrile and amide-hydrolyzing microorganisms. *Biosci. Biotech. Biochem.* **61**: 1419-1427, 1997.
 18. Cohen, M.A., Sawden, J, Turner, N.J. Selective hydrolysis of nitriles under mild conditions by an enzyme. *Tetrahedron Lett.* **31**: 7223-7226, 1990.
 19. Honicke, S., Petra, S., Manfred, P. Enzymatic hydrolysis of nitriles and dinitriles. *J. Chem. Soc. Chem. Commun.* 648-650, 1990.
 20. Cowan, D., Cramp, R., Dereira, R., Graham, D., Almatawah, Q. Biochemistry and biotechnology of mesophilic and thermophilic nitrile metabolizing enzymes. *Extremophiles.* **2**: 207-216, 1998.
 21. Meth-Cohn, O., Wang, M.X. An in-depth study of the biotransformation of nitriles into amides and/or acids using *Rhodococcus rhodochrous* AJ270. *J. Chem. Soc. Perkin-Trans 1*: 1099-1104, 1997.
 22. Beard, T.M., Page, M.I. Enantioselective biotransformations using *Rhodococci*. *Antonie Vanleeuwenhoek.* **74**: 99-106, 1998.
 23. Snell, D., Colby, J. Enantioselective hydrolysis of racemic ibuprofen amide to s-(+)-ibuprofen by *Rhodococcus* AJ270. *Enzyme Microb. Technol.* **24**: 160-163, 1999.

-
24. Masutomo, S., Inoue, A., Kumagai, K., Murai, R., Mitsuda, S. Enantioselective hydrolysis of (R,S) 2-isopropyl 4-chlorophenylacetone nitrile by *Pseudomonas* sp. B21CP. *Biosci. Biotech. Biochem.* **59**: 720-722, 1995.
 25. Fallon, R.D., Stieglitz, B., Turner, Jr. A *Pseudomonas putida* capable of stereoselective hydrolysis of nitriles. *Appl. Microbiol. Biotechnol.* **47**: 156-161, 1997.
 26. Kobayashi, M. Shimizu, S. Metalloenzyme nitrile hydratase: Structure, regulation, and application to biotechnology. *Nature Biotechnol.* **16**: 733-736, 1998.
 27. Kobayashi, M., Fujiwara, Y., Boda M., Komeda, H., Shimizu, S. Identification of active sites in amidase: Evolutionary relationship between amide bond and peptide bond-cleaving enzymes. *Proc. Natl. Acad. Sci. USA.* **94**: 11986-11991, 1997.
 28. Kobayashi, M., Goda, M., Shimizu, S. The catalytic mechanism of amidase also involves nitrile hydrolysis. *FEBS letters.* **439**: 325-328, 1998.
 29. Gibson, G.G., Skett, P. Introduction to drug metabolism, 2nd ed. 1-43, Chapman and Hall, UK, 1994.
 30. Katzung, B.G. Basic and clinical pharmacology. Pp. 34-41, Lange medical publications, USA, 1982.
 31. Silverman, R.B., The Organic Chemistry of Drug Design and Drug Action. 277-350, Academic Press, USA 1992.
 32. Gong, Z.R., Lui, Z., Zhou, H., Cheng, M. Synthesis of CPIN. *Modern Chemical Engineering.* **12**: 32-34, 1998.

